



University of  
**BRISTOL**

## Multicell Beamforming for Cellular Networks

Hannah Andrade Lucki

April 2020

Final year project thesis submitted in support of the degree of  
Bachelor of Engineering in Electrical and Electronic Engineering

Department of Electrical & Electronic Engineering

University of Bristol

## **Declaration and Disclaimer**

Unless otherwise acknowledged, the content of this thesis is the original work of the author. None of the work in this thesis has been submitted by the author in support of an application for another degree or qualification at this or any other university or institute of learning. The views in this document are those of the author and do not in any way represent those of the University.

The author confirms that the printed copy and electronic version of this thesis are identical.

Signed:

A handwritten signature in black ink, appearing to read "Hannah Andrade Lucki".

Hannah Andrade Lucki

Dated: 27/05/2020

## Abstract

The number of wireless devices is predicted to keep growing, with an estimate of 15 connected devices per person by 2030 - according to MarTech Advisor (MTA). This implies that the bandwidth spectrum needed is becoming even higher. High bandwidth demand combined with the increasing throughput requirements of the modern generations of telecommunication systems, such as 4G and 5G, have made beamforming an essential technique for improving bandwidth efficiency. The purpose of beamforming is to improve the link quality by maximising each user's received power while reducing interference, thus enhancing the throughput. Millimeter wave (mmWave) frequency bands are of interest for the next cellular generations: carrier frequencies in these bands are capable of meeting the bandwidth demand to accommodate the emerging data traffic. Beamforming is a particularly appealing way of mitigating the very high-losses experienced by mmWave frequencies through using highly directional narrow beam antennas on one or both ends of the link. These narrow beams, however, pose a challenge in terms of selecting the best beams.

This project focuses on evaluating the benefits of double-directional and transmit beamforming using IEEE 802.15.3c codebooks on a homogeneous cellular network. Several propagation path loss models were considered for different scenarios as a precise estimate of path loss is vital to accurately calculate the link budget. Through the analysis of the results for each configuration generated by the cellular network simulator developed for this thesis, key conclusions were drawn. This was achieved by changing the number of beam patterns ( $K$ ) and antenna elements ( $M$ ), the proportion between them ( $K=2M$  or  $K=M$ ), the beam selection technique used and the ends of the link in which beamforming was implemented (either at the transmitting end or at both transmitting and receiving ends).

It was found that applying uncoordinated beamforming on the transmit side employing  $M=4$   $K=8$  provides an overall improvement of 33.4% in terms of user and cell throughputs in comparison with the isotropic results. The use of  $K=2M$  beam patterns instead of  $K=M$  has also proven to be advantageous for users at the cell-edge as it minimises the gain loss at the intersection of two beams. When assessing double-directional beamforming, the max-SNR and the max-SINR selection methods developed offer a further increase of 15.1% and 17.9% respectively, compared to the average user and cell throughput values obtained with transmit beamforming only.

## Acknowledgements

I would like to express my sincere gratitude and deep appreciation to my supervisor Dr. Simon Armour for his consistent support, patience, guidance, and encouragement. His willingness to give his time so generously has been highly valued. He helped me overcome the academic and personal obstacles I faced throughout this year and I could not have completed my degree without him.

Some special words of gratitude go to my dear friends Yunzhe Wu and Natalia Denysyuk for their unconditional friendship and patience during these three years.

Finally, I sincerely thank my parents Valeria Moreira De Andrade and Joseph Hebert Lucki, my boyfriend Renan Brandão Rambaldi Cavalheiro, my sister Sophia Andrade Lucki and my grandmother Lúcia Moreira De Andrade, for everything.

# Contents

<b>Declaration and Disclaimer .....</b>	<b>ii</b>
<b>Abstract .....</b>	<b>iii</b>
<b>Acknowledgements.....</b>	<b>iv</b>
<b>Contents.....</b>	<b>v</b>
<b>List of Acronyms.....</b>	<b>vii</b>
<b>Chapter 1. Introduction.....</b>	<b>1</b>
1.1. Motivation & Objectives .....	1
1.2. Contributions .....	2
1.3. Outline of Thesis .....	4
<b>Chapter 2. Background.....</b>	<b>5</b>
2.1. Receiver Noise Input Power.....	5
2.2. SNR .....	5
2.3. SINR .....	6
2.4. Bandwidth Efficiency .....	7
2.5. Throughput .....	7
2.6. Link Budget & Received Signal Power.....	8
2.7. Cellular Networks.....	8
2.8. Path Loss Propagation Models .....	10
2.8.1. Free Space Path Loss Model (FSPL).....	10
2.8.2. Okumura-Hata Model.....	11
2.8.3. Cost231-Hata Model .....	12
2.8.4. Cost231-Walfisch-Ikegami Model.....	13
2.8.5. Stanford University Interim (SUI).....	16
2.8.6. ECC-33 .....	17
2.9. Beamforming Codebooks .....	18
2.9.1. IEEE 802.15.3c .....	18
<b>Chapter 3. The Cellular Network Simulator.....</b>	<b>22</b>
3.1. Outline .....	22
3.2. Cell Deployments .....	24
3.3. Flowchart .....	25
3.3.1. Generate network scenario: cells, BSs, UEs and uniformly random distributed UE coordinates.....	26
3.3.2. Calculate distance between each UE and BS of cell of interest & between each UE and each interfering BS.....	27
3.3.3. Calculate path losses .....	28
3.3.4. Calculate angles between BS of cell of interest and each UE .....	28

3.3.5.	Apply 3c beamforming codebook using M antenna elements and K beam patterns / Obtain Array Gain for each individual UE and Array Gain of interfering BSs.....	28
3.3.6.	Calculate Prx, SNR, Interference, Bandwidth Efficiency, User Throughput, Cell Throughput .....	29
3.4.	Monte Carlo passes.....	30
3.5.	List of Assumptions .....	31
3.6.	Macrocell Simulation Scenario .....	32
3.7.	Microcell Simulation Scenario.....	33
3.8.	mmWave Picocell Simulation Scenario.....	35
<b>Chapter 4.</b>	<b>Transmit Beamforming.....</b>	<b>36</b>
4.1.	Transmit Beamforming Cases .....	37
4.2.	Results.....	39
4.3.	Conclusion.....	42
<b>Chapter 5.</b>	<b>The Impact of Basestation Antenna Configurations on Transmit Beamforming .....</b>	<b>43</b>
5.1.	Beam Pattern Selection & Highest Antenna Array Gain .....	43
5.2.	Results.....	45
5.3.	Conclusion.....	48
<b>Chapter 6.</b>	<b>Double-Directional Beamforming.....</b>	<b>49</b>
6.1.	Results.....	50
6.2.	Conclusion.....	52
<b>Chapter 7.</b>	<b>Conclusions .....</b>	<b>54</b>
7.1.	Future Work .....	55
<b>Mitigation plan.....</b>		<b>57</b>
<b>References .....</b>		<b>58</b>
<b>Appendix A.</b>	<b>Macrocell simulation.....</b>	<b>63</b>
<b>Appendix B.</b>	<b>Microcell simulation .....</b>	<b>66</b>
<b>Appendix C.</b>	<b>Array Factors polar plots .....</b>	<b>69</b>
<b>Appendix D.</b>	<b>Software Traceability.....</b>	<b>71</b>

## **List of Acronyms**

BS	Basestation
UE	User Equipment
SUI	Stanford University Interim
DL	Downlink
SNR	Signal-to-Noise Ratio
SINR	Signal-to-Interference-Plus-Noise Ratio
Tx	Transmitter
Rx	Receiver
AWGN	Additive Whit Gaussian Noise
mmWave	Millimetre Wave
MIMO	Multiple-Input Multiple-Output
MISO	Multiple-Input Single Output
LTE	Long Term Evolution
CDMA	Code Division Multiple Access
OFDMA	Orthogonal Frequency Division Multiple Access
SC-FDMA	Single Carrier Frequency Division Multiple Access
CDF	Cumulative Distribution Function
LoS	Line of Sight
Non-LoS	Non Line of Sight
ECC	Electronic Communications Committee
PL	Path Loss

# **Chapter 1.**

## **Introduction**

Cellular Networks are essential to society, especially now (2020, COVID-19) as being connected became more important than ever – proof of this is the unprecedented network traffic congestion suffered during this period.

So far, five generations of cellular networks exist. The first cellular network generation, 1G, was launched in the early 1980s and had the basic mobile voice services, using analogue-based protocols. The second generation, 2G, introduced capacity and coverage through digital standards such as GSM, CDMA, and IS-95 [1]. 3G was announced in the 2000s and was still mostly dominated by CDMA, but it added mobile broadband, improved voice service quality, and increased the speed. 4G was introduced in 2008, with two main technologies: WiMAX, based on OFDMA, and LTE, standardized by the 3G Partnership Program using OFDMA and SC-FDMA [2]. The most recent generation, 5G, has finished its standardization activities in 2020 [3].

According to Cisco's Annual Report (2018-2023), 10% of the global mobile connections will have migrated to 5G, the fifth and newest generation of cellular networks, by 2023, with its speed being expected to be nearly 13 times faster than 4G. Sub-6GHz are suffering from limited (shortage) spectrum availability [4], hence the need to look for other potential frequency bands. mmWave frequency bands are a very promising candidate that can support higher bandwidths to meet 5G's needs, with beamforming at 28 GHz frequency being analysed on this project.

### **1.1. Motivation & Objectives**

Beamforming was included in 5G specifications [5], evidencing that this technique is essential to support the new cellular generation: it improves link performance since it achieves higher bandwidth efficiency and hence higher throughput that meets this ever-increasing demand [6]. The ultimate goal of this project is to explore beamforming as a solution to enhance the throughput by addressing the challenge of selecting the best beam pattern.

mmWave frequencies result in extremely high path losses – which can be compensated using beamforming, but on the other hand frequencies in this band physically reduce the size of antennas and the uniform spacing between antennas. This is because distance the between antenna elements in an array depends on the wavelength. Wavelengths are shorter at frequencies as high as mmWaves, facilitating the implementation of antenna arrays with larger numbers of elements [5] and thus narrower beams [7].

Taking the mmWave challenges into consideration and the possible beamforming configurations, the main aims of this thesis are:

- Develop a software simulator of cellular networks.
- Measure and compare performance metrics.
- Analyse the influence of path loss propagation model selection on these metrics.
- Study the impact of the parameters of a cellular network on the performance metrics.
- Create transmit beamforming cases to model the antenna gain of transmit antennas according to the technique of selecting beams for transmit beamforming.
- Examine the benefits of transmit codebook 3c (IEEE 802.15.3c) beamforming.
- Investigate the effect of varying the number of antenna elements ( $M$ ), the number of beam patterns ( $K$ ) and their relationship ( $K=M$  or  $K=2M$ ).
- Evaluate the advantages of double-directional beamforming.

## 1.2. Contributions

The first contribution of this thesis is the user-friendly software simulator of hexagonal (homogenous) cellular networks, which was fully developed by the author. It provides results in several forms to facilitate interpretation such as histograms, minimum/mean/maximum bar plots, CDF and heat plots. It calculates the following performance metrics: SNR, SINR, User Throughput and Cell Throughput. Furthermore, the simulator offers 7 options of propagation path loss models and customisable cellular network parameters. The software's code was structured to accommodate

future changes. Thus, this software can support other research – it can easily be modified to explore new topics of cellular networks. Additionally, the developed software can be used as a learning tool.

The second contribution is the original idea of cases of beam selection for transmit beamforming, which were implemented as part of the software simulator. Four cases were developed: the first case is overly optimistic and provides an upper bound in terms of performance metric. The second one shows how randomness can deteriorate the performance. The third and fourth cases are versions of uncoordinated beamforming, with the latter being the most realistic. All cases involved IEEE 802.15.3c beamforming applied to all basestations.

After selecting the “case” that best fits uncoordinated beamforming, the influence of the number of antenna elements ( $M$ ) and number of beam patterns ( $K$ ) was investigated by applying various  $M$  and  $K$  values in a similar manner, using  $K=M$  and  $K=2M$ . It was shown that the improvement for SNR from  $K=M$  to  $K=2M$  is more significant when using larger  $M$ ’s, indicating that narrower beams (larger  $M$ ’s) can benefit more from better precision offered by  $K=2M$  beam patterns.

Two approaches were created for determining the optimal beam pair in a double-directional beamforming scenario: a max-SINR method and a max-SINR exhaustive search. Adding receive beamforming on top of transmit beamforming to achieve double-directional beamforming was found to be more worthwhile than increasing  $M$  on the transmitter side for transmit beamforming.

The third contribution consists of the discoveries and conclusions drawn from this research. These conclusions are supported by comparison of improvements in terms of percentage relative to the isotropic results, highlighting to a network engineer which beamforming configuration is more adequate for improving which metrics and always underlining at what cost.

### **1.3. Outline of Thesis**

Chapter 2 introduces the principles of cellular networks, including performance metrics and how they are obtained. It summarises several Path Loss Models and explains the concept of beamforming.

Chapter 3 describes the Cellular Network simulator and its functionality. This chapter includes a list of assumptions valid for the analysis and a flow-chart of the simulation process. The steps of the flowchart are rationalised, mentioning the equations used in the software code. It presents the first analysis of this dissertation, which focuses on Path Loss Models of the three simulation scenarios displayed in the list of assumptions.

Chapter 4 focuses on the four cases of beam selection for transmit beamforming. It analyses how each case has implications on the performance metrics and their authenticity. It also explains the concepts of the switched beamforming technique used.

Chapter 5 applies one of the cases studied in Chapter 4 – the case considered the most realistic. It explores the impact of changing the values of antenna elements, and beampatterns as well as the influence of their relationship ( $K=M$  and  $K=2M$ ) on the performance metrics.

Chapter 6 investigates the additional benefits of implementing receive beamforming to the existing transmit beamforming, making it a double-directional beamforming system. It applies two types of beam selection: a max-SNR method and a max-SINR exhaustive search.

Chapter 7 outlines and discusses the main points from each chapter. It also provides opportunities for future research topics.

# Chapter 2.

## Background

This chapter introduces the reader to the principles of cellular networks and explains the performance metrics and their equations. This knowledge is needed to follow the analysis conducted throughout the thesis.

### 2.1. Receiver Noise Input Power

The noise floor of the receiver determines lowest amount of signal received that can be detected (distinguished from noise) [8]. The model of noise in a receiver is assumed to be the Additive White Gaussian Noise (AWGN). It can be calculated as the sum of the thermal noise, which is the noise created by the movement of electrons in conducting media [9], and the noise figure.

$$N(\text{dBm}) = 10\log_{10}\left(\frac{kTB}{10^{-3}}\right) + NF = -174\text{dBm} + 10\log_{10}B + \text{NF} \quad (1)$$

Where  $N$  is the receiver noise input power [10] in dBm,  $k$  is the Boltzmann constant ( $1.3807 \times 10^{-23} \text{ J/K}$  in MATLAB),  $T$  is the temperature in Kelvin which is standardized as  $290K$ ,  $B$  is the channel bandwidth in Hz,  $kTB$  is the thermal noise which is equivalent to  $-173.9752 \text{ dBm/Hz}$  and is therefore the amount of noise in 1Hz bandwidth at room temperature.  $NF$  is the noise figure in dB, which has been set as 10dB for this dissertation [11].

### 2.2. SNR

SNR is the signal-to-noise ratio. Signal strength is the transmitter power minus losses, therefore signal strength is equivalent to the received power. It measures how much received power is necessary in relation to the noise in order to guarantee detection.

$$\text{SNR} = \frac{S}{N} \quad (2)$$

$$\text{SNR(dB)} = 10\log_{10}\frac{S}{N} \quad (3)$$

## 2.3. SINR

Signal-to-interference-plus-noise-ratio accounts for the interference experienced by a user. The efficiency and throughput of a communication system are directly related to the receiver's SINR, therefore it is important to maximise it as much as possible. This measure can be expressed linearly or in decibels.

$$SINR = \frac{S}{I + N} \quad (4)$$

$$SINR(dB) = 10 \log_{10} \frac{S}{I + N} \quad (5)$$

$$SINR_{BS_o,U} = \frac{\frac{P_{tx}}{PL_{BS_o,U}} G_{BS_o,U}}{\sum_{BS_i \neq BS_o} \frac{P_{tx}}{PL_{BS_i,U}} G_{BS_i,U} + N} = \frac{P_{rx_{BS_o,U}}}{\sum_{BS_i \neq BS_o} P_{rx_{BS_i,U}} + N} \quad (6)$$

Where S is the signal power, which is the received power  $P_{rx}$  of the central cell, in Watts – it is further discussed in Section 2.6. N is the receiver input noise power in Watts – discussed in Section 2.1. I is the interference power, which is equivalent to the sum of the received powers from the other cells, in Watts.  $BS_o$  represents the transmitter of the central cell and U is the receiver (each user has a receiver) and  $BS_i$  stands for the interfering link (one of the six cochannel cells).  $P_{tx}$  is the transmitted power, G is the beamforming gain and PL is the path loss between the receiver U and transmitter BS [12], all in Watts – these 3 terms are used to calculate the received power in terms of Watts.

Intercell interference is one of the main causes of low SINRs - one way of minimising interference from neighbouring cells is by increasing the distance between co-channel cells, known as reuse distance [13]. For this thesis, the interference is assumed to come from the first-tier cochannel cells (the six cells that surround the central cell) as interference from second and higher tiers is usually equivalent to less than 1% of the total interference [14].

## 2.4. Bandwidth Efficiency

Bandwidth efficiency (or spectral efficiency) measures how effectively the frequency spectrum is used to achieve high data rates. Therefore, bandwidth efficiency evaluates the number of bits per second successfully transmitted per Hz [15].

The Shannon-Hartley Capacity theorem calculates the maximum theoretical capacity or maximum data rate transmitted from base station to user [15]. Shannon uses SNR (instead of SINR) for the calculation of bandwidth efficiency, so both equation (7) and (8) are adapted versions using linear SINR in which the interference is assumed to resemble noise. The bandwidth efficiency is calculated in bits/s/Hz as follows:

$$\eta_B = \log_2(1 + SINR) \quad (7)$$

## 2.5. Throughput

The throughput – a more realistic capacity – is calculated using an adapted Shannon-Hartley Capacity theorem, as mentioned previously mentioned. The user throughput is the data rate that can be supported by a user. This metric can be calculated using the following equation:

$$C_{user} = B_{user} \log_2(1 + SINR) = \eta_B B_{user} \quad (8)$$

$C_{user}$  is the user throughput in Mbits/s, SINR is linear, and  $B_{user}$  is the user bandwidth in MHz, which can be calculated by dividing the cell bandwidth  $B_{cell}$  in MHz by the number of users.

The cell throughput can be computed by summing all the user throughputs of each user in the cell:

$$C_{cell} = \sum_{user=1}^{number\ of\ users} C_{user} \quad (9)$$

The cell throughput is not an indicator of fairness between users as it only displays the results of the entire cell, hence the need to consider both cell and user throughput. The user throughput helps analyse the fairness amongst users (e.g.: a high cell throughput is not a good indicator if some users have a very low user throughput and some have high).

## 2.6. Link Budget & Received Signal Power

The link budget relates the power at the receiver to the power at the transmitter, considering all the gains and losses in the propagation medium from the transmitter to the receiver. It is used to estimate the received power [16], which is a crucial parameter to compute the SNR and SINR [17]. The received signal power can be expressed as [18]:

$$P_{rx} = \frac{P_{tx}G_{tx}G_{rx}}{PL} \quad (10)$$

$$P_{rx}(dBm) = P_{tx} + G_{tx} + G_{rx} - PL \quad (11)$$

Where  $P_{tx}$  is the base station transmit power in dBm,  $G_{tx}$  is the gain of the transmitter antenna in dBi and their sum ( $P_{tx} + G_{tx}$ ) forms the Equivalent Isotropic Radiated Power (EIRP) in dBm.  $G_{rx}$  is the receiver antenna gain in dBi and  $PL$  is the path loss in dB.  $PL$  varies according to the chosen Path Loss Propagation Model as different parameters are taken into account. In (10), all the terms are expressed in Watts.

## 2.7. Cellular Networks

The basic premise behind cellular systems is to explore power falls off with distance (path loss) to reuse the same frequency at spatially separated locations [19]. The coverage area of a cellular network is divided into non-overlapping cells and each cell covers a hexagon.

Hexagons are traditionally used to represent the area covered by a basestation as they can tessellate, which makes it a more efficient design than other polygons such as squares or triangles. Hexagons provide a better approximation to the actual coverage [2].

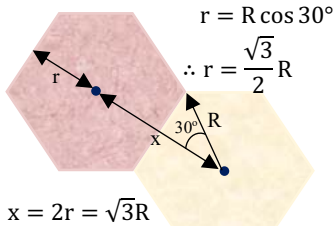


Figure 1 – Distance between cell centres. Image created by the author and inspired by [2].

Reuse distance,  $D$ , is the distance between co-channel cells (cells using the same frequencies) and it is directly proportional to the cluster size. For a cluster size of 1,  $D = x = 2r = \sqrt{3}R$ , where  $x$  is the centre-to-centre distance between adjacent channels,  $r$  is the apothem (centre to mid-point of a side) of the hexagon and  $R$  is the radius of the hexagon.

Cluster sizes are represented by the letter N. The radio resources available are equally shared by N cells. A low N represents a higher overall capacity (at the cost of higher interference) - more bandwidth available in each cell, so it can accommodate more users per cell. Cluster sizes  $>1$  do not allow neighbouring cells to use the same set of frequencies as a way of preventing interference. As  $N=1$  for this thesis, this is beyond the spectrum.

To determine the SNR, only the distance between the user of interest and the basestation of cell of interest (central cell) needs to be calculated and then applied to the path loss to calculate the link budget and find the received power, which then is divided by noise.

In order to find the SINR, the distances between the user of interest and each of the co-channel basestations are also required to calculate the path loss needed at the link budget to find the sum of interference coming from co-channel cells. The received power is divided by the noise plus the sum of interference.

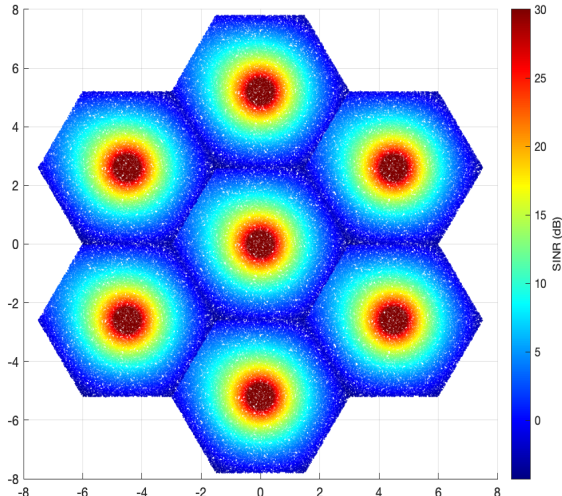


*Figure 3 - Macrocell isotropic Okumura-Hata SINR heat map. Simulation results generated by the author's simulator. Idea inspired by [67]*

interference when the distance from the UE to its BS and from the UE to an interfering BS is the same or almost the same, which is true for UEs at cell-edge.

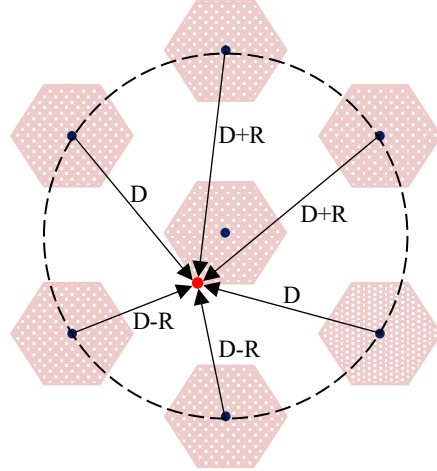


*Figure 2 - Co-channel interference in the worst case for Downlink: when the UE (red dot) is at cell-edge. Cluster size of N=7. Image created by the author and inspired by*

Co-channel interference is caused by signals transmitted by another cell using the same radio spectrum. The results in Figure 3 show that the UEs further away from their BS have lower Signal-to-Interference-Plus-Noise Ratio. This is a result of increased path loss with distance, weakening the received signal, and also the fact that users at cell-edge suffer the most from inter-cell interference. As the cluster size is one, every neighbouring cell is using the same frequency resources, so they are all interferers, resulting in increased inter-cell

Increasing the signal power (received power  $P_{rx}$ ) by boosting the transmitted power  $P_{tx}$  would initially seem like a logical solution to solve the low SINR at cell-edges and it does work for noise-limited networks, but not for interference-limited ones. In an interference-limited situation, this approach would increase the interference as it increases the  $P_{rx}$  not only of the cell of interest, but of all the interfering cells too, hence the SINR of users at cell-edge would not be improved [20] [21].

	<b>SNR (dB)</b>	<b>SINR (dB)</b>	<b>Spectral Efficiency (bps/Hz)</b>	<b>User throughput (Mbits/sec)</b>
<b>User at cell-centre (x=0.0161, y=0.0147)</b>	100.1551	30	9.9672	0.8306
<b>User at cell-edge (x=-1.4857, y=-2.5934)</b>	25.9702	-4.2540	0.4599	0.0383

*Table 2-1 - Metrics obtained from isotropic macrocell simulation for user at the cell centre and user at the cell edge selecting Okumura-Hata model. Table created by the author using simulation results, idea inspired by [22].*

## 2.8. Path Loss Propagation Models

As no single model is appropriate for all the different environments, examining the possible path loss propagation models is of uttermost importance to determine the most suitable option, which should provide the most accurate path loss value and consequently, enable the calculation of a more precise value of received power  $P_{rx}$ .

### 2.8.1. Free Space Path Loss Model (FSPL)

This is a theoretical model. It measures the disparity between the power transmitted and the power received without evaluating attenuation due to physical properties - it assumes no obstacles [23]. Free Space Path Loss depends on two parameters: the carrier frequency and the distance between the receiver and transmitter. This model is only valid for signal attenuation with line of sight (LoS) scenarios and it is generally used for isotropic antennas (antenna gain is equal to unity) [2]. FSPL is expressed in decibels (dB) as below:

$$PL_{fs}(dB) = FSPL = 10 \log \left( \frac{4\pi d}{\lambda} \right)^2 = 10 \log \left( \frac{4\pi f_c d}{c} \right)^2 \quad (12)$$

Where  $\lambda$  is the carrier wavelength in meters (from  $\lambda = c/f_c$ ),  $f_c$  is the carrier frequency in Hz,  $c$  is the speed of light in meters per second (299792458m/s on MATLAB), and  $d$  is the distance between the transmitter antenna and receiver antenna in meters. For  $f_c$  in MHz and  $d$  in kilometres, (12) is adjusted to:

$$PL_{fs}(dB) = 20 \log_{10} d + 20 \log_{10} f_c + 32.44 \quad (13)$$

As seen on Figure 1, the Free Space Path Loss is proportional to the square of the carrier frequency, showing that the loss is much more critical for mmWave frequencies (between 24GHz and 100GHz).

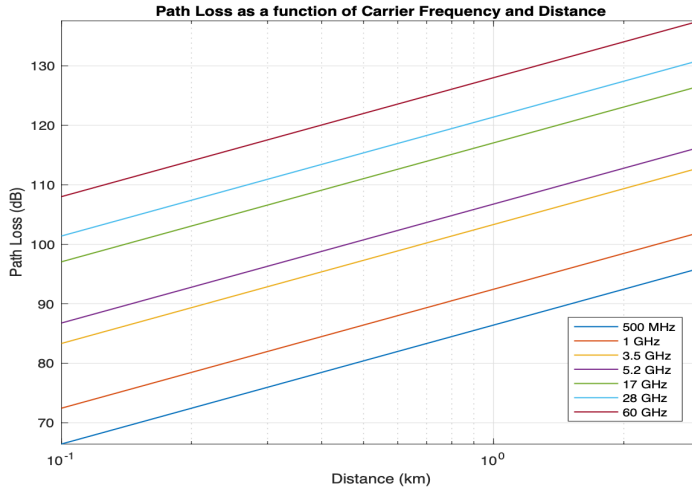


Figure 4 - Path Loss as a function of Carrier Frequency and Distance. Results generated using the author's simulator, idea inspired by [2].

### 2.8.2. Okumura-Hata Model

This empirical model was established in Japan and can be applied to urban areas as well as suburban and open areas. It is restricted in terms of parameters such as carrier frequency ( $f_c$ ), height of transmitter ( $h_{tx}$ ) and receiver ( $h_{rx}$ ) antennas and distance between these antennas ( $d$ ). It is often used for estimating the path loss for macrocells considering its valid separation distance range. The model is valid for the following parameter ranges [14]:

Carrier frequency $f_c$ (MHz)	<b>150 ≤ <math>f_c</math> ≤ 1500 MHz</b>
Distance from basestation to user $d$ (km)	<b>1 ≤ <math>d</math> ≤ 20 km</b>
Transmitter antenna height $h_{tx}$ (m)	<b>30 ≤ <math>h_{tx}</math> ≤ 200 m</b>
Receiver antenna height $h_{rx}$ (m)	<b>1 ≤ <math>h_{rx}</math> ≤ 10 m</b>

Table 2-2: Okumura-Hata's valid parameters table

The path loss between two antennas for an urban area is given by the equation [24] [25]:

$$PL_{OH\_Urban}(dB) = 69.55 + 26.16 \log_{10} f_c - 13.82 \log_{10} h_{tx} - a(h_{rx}) + (44.9 - 6.55 \log_{10} h_{tx}) \log_{10} d \quad (14)$$

For a suburban area and for an open area, it is modified by adding extra terms, as shown in equations (15) and (16):

$$PL_{OH\_Suburban}(dB) = PL_{OH\_Urban}(dB) - 5.4 - 2(\log_{10}(f_c/28))^2 \quad (15)$$

$$PL_{OH\_OpenArea}(dB) = PL_{OH\_Urban}(dB) - 40.94 - 4.78(\log_{10} f_c)^2 + 18.33 \log_{10} f_c \quad (16)$$

Where  $a(h_{rx})$  is the correction factor in dB for the receiver antenna height.

$$a(h_{rx}) = \begin{cases} 0.8 - 1.56 \log_{10} f_c + (1.1 \log_{10} f_c - 0.7)h_{rx} & \text{for small/medium city} \\ 8.29(\log_{10}(1.54h_{rx}))^2 - 1.1 & \text{for } f_c \leq 300 \text{ MHz} \\ 3.2(\log_{10}(11.75h_{rx}))^2 - 4.97 & \text{for } f_c \geq 300 \text{ MHz} \\ & \text{for large city} \end{cases}$$

### 2.8.3. Cost231-Hata Model

Based on measured data, this model is considered an extension of the Okumura-Hata model. Cost231-Hata model can predict the path losses of higher carrier frequencies:  $1500 \leq f_c \leq 2000 \text{ MHz}$  [26], which includes the 3G band. The suitable range of the other parameters (except for the carrier frequency) remains the same as for the Okumura-Hata model (Table 2-2) and so does the correction factor for the receiver antenna height,  $a(h_{rx})$ .

The path loss equation is

$$PL_{C231H}(dB) = 46.3 + 33.9 \log_{10} f_c - 13.82 \log_{10} h_{tx} - a(h_{rx}) + (44.9 - 6.55 \log_{10} h_{tx}) \log_{10} d + C \quad (17)$$

Where C is the correction factor in dB for the area.

$$C = \begin{cases} 0 & \text{for medium city/urban areas} \\ & \text{with moderate tree density} \\ 3 & \text{for metropolitan centre} \end{cases}$$

#### 2.8.4. Cost231-Walfisch-Ikegami Model

The Cost231-Walfisch, unlike the non-theoretical models previously discussed, is valid for smaller cells as it has a lower restriction in terms of distance – it can be used as a micro-cell model [24]. For distances smaller than the stipulated (0.02 km), the Free Space Path Loss should be used.

- i) LoS (Line-of-Sight)

Line-of-Sight assumes no obstacles between the transmitter and receiver antenna. The parameters should be within the ranges:

Carrier frequency $f_c$ (MHz)	<b>800 ≤ <math>f_c</math> ≤ 2000 MHz</b>
Distance from basestation to user $d$ (km)	<b>0.02 ≤ <math>d</math> ≤ 5 km</b>

Table 2-3 –LoS Cost231-Walfisch-Ikegami's valid parameters table

This path loss equation of this model is:

$$PL_{C231WI-Los}(dB) = 42.6 + 26 \log_{10} d + 20 \log_{10} f_c \quad (18)$$

The value of 42.6 was chosen so that  $PL_{C231WI-Los}(dB)$  is equivalent to the Free Space Path Loss (FSPL) calculated using a distance of  $d = 0.02 \text{ km}$  [27].

- ii) Non-LoS

This version of the semi-deterministic model [28] takes into account losses due to obstacles when calculating the path loss – these are represented by  $L_{msd}$  and  $L_{rts}$ , which are the multi-screen diffraction loss and the roof-to-street diffraction and scatter loss respectively. The valid parameters are [24]:

Carrier frequency $f_c$ (MHz)	<b>800 ≤ <math>f_c</math> ≤ 2000 MHz</b>
Distance from basestation to user $d$ (km)	<b>0.02 ≤ <math>d</math> ≤ 5 km</b>
Transmitter antenna height $h_{tx}$ (m)	<b>4 ≤ <math>h_{tx}</math> ≤ 50 m</b>
Receiver antenna height $h_{rx}$ (m)	<b>1 ≤ <math>h_{rx}</math> ≤ 3 m</b>

Table 2-4 - Non-LoS Cost231-Walfisch-Ikegami's valid parameters table

As illustrated below,  $h_{Roof}$  is the roof height of buildings in meters,  $\Delta h_{tx}$  is the height of the transmitter antenna in relation to the rooftop's height in meters,  $\Delta h_{rx}$  is the height of the receiver antenna in relation to the height of the rooftops in meters,  $b$  is the distance between buildings in meters and  $w$  is the width of the streets, and  $\phi$  is the orientation of the road in terms of direct path in degrees.

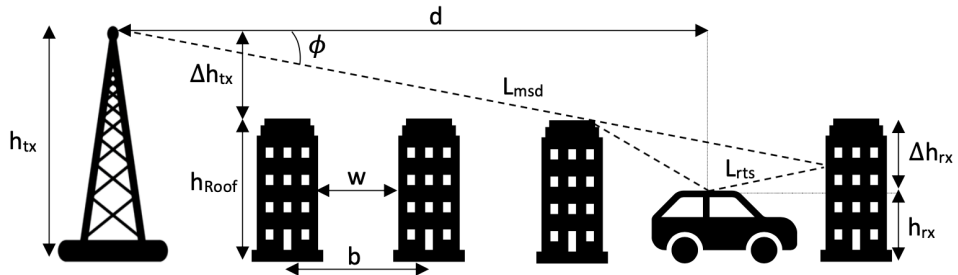


Figure 5 – Geometry of Cost231-Walfisch-Ikegami. Image created by the author and inspired by [29].

The standard value of roof height is  $h_{Roof} = 3 \times \text{number of floors} + \text{roof}$ . The value of *roof* is 3 meters if pitched and 0 meters if flat. The height of the transmitter antenna in relation to the height of the rooftops in meters is the difference between heights:  $\Delta h_{tx} = h_{tx} - h_{Roof}$ . Similarly,  $\Delta h_{rx} = h_{rx} - h_{Roof}$ . The non-LoS model presents good results particularly for  $h_{tx} \gg h_{Roof}$ . Errors can be expected when these two heights are similar,  $h_{tx} \approx h_{Roof}$ . This model is not recommended for scenarios in which  $h_{tx} \ll h_{Roof}$  [30], as it can result in path loss overestimation.

The value of  $b$ , the uniform building separation, is within the range of 20 and 50 m. The width of the streets is half of the building separation,  $w = \frac{b}{2}$  (m). Ideally, the value of the road orientation angle  $\phi$  is 90°.

The non-LoS Cost231-Walfish-Ikegami path of loss is dependent on the sum of losses

$$PL_{C231WI-nonLoS}(dB) = \begin{cases} L_o + L_{rts} + L_{msd} & \text{for } L_{rts} + L_{msd} \geq 0 \\ L_o & \text{for } L_{rts} + L_{msd} < 0 \end{cases} \quad (19)$$

$L_o$  is the Free Space Path Loss (FSPL). Thus, it can be expressed as

$$L_o = FSPL = 32.4 + 20 \log_{10} d + 20 \log_{10} f_c \quad (20)$$

$L_{rts}$ , the roof-to-street diffraction and scatter loss, can be calculated as follows

$$L_{rts} = -16.9 - 10 \log_{10} w + 10 \log_{10} f_c + 20 \log_{10} \Delta h_{rx} + L_{ori} \quad (21)$$

Where  $L_{ori}$  is the orientation loss:

$$L_{ori} = \begin{cases} -10 + 0.354(\phi), & 0 \leq \phi \leq 35^\circ \\ 2.5 + 0.075(\phi - 35^\circ), & 35^\circ \leq \phi \leq 55^\circ \\ 4 - 0.114(\phi - 55^\circ), & 55^\circ \leq \phi \leq 90^\circ \end{cases} \quad (22)$$

The multi-screen diffraction loss,  $L_{msd}$ , is composed by other factors.

$$L_{msd} = L_{bsh} + k_a + k_d \log_{10} d + k_{f_c} \log_{10} f_c - 9 \log_{10} b \quad (23)$$

$L_{bsh}$  is the negative loss (gain) due to shadowing as the transmitter antenna height exceeds the height of rooftop.  $k_a$  accounts for the increase in path loss resulting from transmitter antennas heights exceeding the rooftops heights of other buildings.

$$L_{bsh} = \begin{cases} -18 \log_{10}(1 + \Delta h_{tx}) & \text{for } h_{tx} > h_{Roof} \\ 0 & \text{for } h_{tx} \leq h_{Roof} \end{cases} \quad (24)$$

$$k_a = \begin{cases} 54, & h_{tx} > h_{Roof} \\ 54 - 0.8\Delta h_{tx}, & d \geq 0.5km \text{ and } h_{tx} \leq h_{Roof} \\ 54 - 0.8\Delta h_{tx}d/0.5 & d < 0.5km \text{ and } h_{tx} \leq h_{Roof} \end{cases} \quad (25)$$

$k_d$  regulates the dependency of  $L_{msd}$  on distance and  $k_{f_c}$  regulates its dependency on the carrier frequency.

$$k_d = \begin{cases} 18, & h_{tx} > h_{Roof} \\ 18 - 15\Delta h_{tx}/h_{Roof}, & h_{tx} \leq h_{Roof} \end{cases} \quad (26)$$

$$k_f = -4 + \begin{cases} 0.7(f_c/925 - 1), & \text{suburban} \\ 1.5(f_c/925 - 1), & \text{urban} \end{cases} \quad (27)$$

### 2.8.5. Stanford University Interim (SUI)

This model was developed by the Stanford University, focusing on carrier frequencies below 11GHz. The SUI model can be modified and extended so that it extends to new millimeter wave (mmWave) cellular systems as in [31]. It has been proven that this model provides accurate results for carrier frequencies between 2.5GHz and 2.7GHz and the model is valid for [25]:

Carrier frequency $f_c$ (MHz)	<b>1900 ≤ <math>f_c</math> ≤ 3500 MHz</b>
Cell radius $R$ (km)	<b>0.1 ≤ <math>R</math> ≤ 8 km</b>
Transmitter antenna height $h_{tx}$ (m)	<b>10 ≤ <math>h_{tx}</math> ≤ 80 m</b>
Receiver antenna height $h_{rx}$ (m)	<b>2 ≤ <math>h_{rx}</math> ≤ 10 m</b>

Table 2-5 – Stanford University Interim valid parameters table

This empirical model can portray three types of terrain: A, B and C. Terrain A describes hilly area with moderate/very dense foliage, and it presents the maximum path loss. Terrain B suits hilly regions with few trees or flat terrains with moderate/heavy tree concentrations. Terrain C is used for flat terrains with light foliage – it has the minimum path loss [32].

The path loss equation contains several correcting factors and it is only applicable for  $d > d_o$ , where  $d_o = 0.1 \text{ km}$ . In equation (29),  $\lambda$  is the wavelength in meters.

$$PL_{SUI} = FSPL_{d_o} + 10\gamma \log_{10} \frac{d}{d_o} + X_{f_c} + X_{h_{rx}} + S \quad (28)$$

$$FSPL_{d_o} = 20 \log \left( \frac{4\pi d_o}{\lambda} \right) \quad (29)$$

$X_{f_c}$  is the correction factor for frequencies above 2000 MHz.  $X_{h_{rx}}$  is the correction factor for the receiving antenna height in meters.  $S$  is the correction factor for shadowing in dB, which is in the range between 8.2 (for rural) and 10.6 dB (for urban).

$$X_{f_c} = 6 \log_{10}(f_c / 2000) \quad (30)$$

$$X_{h_{rx}} = \begin{cases} -10.8 \log_{10}(h_{rx} / 2000) & \text{for terrain type A and B} \\ -20 \log_{10}(h_{rx} / 2000) & \text{for terrain type C} \end{cases} \quad (31)$$

$$\gamma = a - bh_{tx} + \left( \frac{c}{h_{tx}} \right) \quad (32)$$

$\gamma$  is the path loss exponent. For LoS (FSPL),  $\gamma=2$  and for urban environments,  $3 \leq \gamma \leq 5$ . The values for  $a$ ,  $b$  and  $c$  can be defined according to the terrain and are displayed on the table below:

	$a$	$b (m^{-1})$	$c (m)$
Terrain A	4.6	0.0075	12.6
Terrain B	4	0.0065	17.1
Terrain C	3.6	0.005	20

Table 2-6 – Table of  $a$ ,  $b$  and  $c$  values. Source: [33]

A modified version of the SUI model appropriate for mmWave frequency bands was developed in [34]:

$$PL_{SUI,mod} = \alpha_{NLOS} \times (PL_{SUI}(d) - PL_{SUI}(d_o)) + S \quad (33)$$

Where  $\alpha_{NLOS}$  is the mean slope correction factor. For 28GHz, if the value of  $h_{tx}$  is closer to 7m than it is to 17m, then  $S = 10.8$  and  $\alpha_{NLOS} = 0.71$ . Otherwise, the values assigned are  $S = 7.4$  and  $\alpha_{NLOS} = 0.88$ .

### 2.8.6. ECC-33

This model was developed by the Electronic Communications Committee (ECC), hence the name. It is essentially a modified version of the Okumura model, adapted to represent a fixed wireless access (FWA) system. [35] The ECC-33 model can accommodate carrier frequencies within the range of  $700 \leq f_c \leq 3500$  MHz – it is important to highlight that the frequencies in the equations related to this model are in GHz, not in MHz.

$$PL_{ECC-33}(dB) = A_{fs} + A_{bm} - G_{tx} - G_{rx} \quad (34)$$

Where  $A_{fs}$  is the free-space attenuation,  $A_{bm}$  is the basic median path loss,  $G_{tx}$  is the transmitter antenna height gain factor and  $G_{rx}$  is the receiver antenna height gain factor. These can be expressed by the following equations, respectively:

$$A_{fs} = FSPL = 92.4 + 20 \log_{10} d + 20 \log_{10} f_c \quad (35)$$

$$A_{bm} = 20.41 + 9.83 \log_{10} d + 7.89 \log_{10} f_c + 9.59 [\log_{10} f_c]^2 \quad (36)$$

$$G_{tx} = \log_{10} \frac{h_{tx}}{200} [13.98 + 5.8 (\log_{10} d)^2] \quad (37)$$

$$G_{rx} = [42.57 + 13.7 \log_{10} f_c] [\log_{10} h_{rx} - 0.585] \quad (38)$$

## 2.9. Beamforming Codebooks

Codebook-based beamforming can mitigate the considerably high path-losses of mmWaves [36] [37] which were mentioned in Section 2.8.1. Beamforming aims at maximising each user's received power  $P_{rx}$  whilst minimising the other user's interference, boosting the throughput [4]. It reduces the power consumption as the signal is guided to a specific direction through narrow beams, instead of transmitting it in all directions as it was with isotropic antennas [38]. These narrow beams are generated by multiple antennas elements. When a pair of beams is chosen - one beam chosen at the receiver and another beam is chosen at the transmitter – such that it maximises the link quality, this pair of beams is considered an optimal pair.

Codebook refers to a matrix containing several sets of antenna weighting coefficients. A matrix beamforming codebook has a size of  $M \times K$ , where  $M$  is the number of antenna elements and  $K$  is the number of beam patterns generated by the codebook [39]. For a 1-D phased antenna array, the uniform spacing  $d$  is  $\lambda/2$  where  $\lambda$  is the carrier wavelength in meters. Codebook is a matrix [40]:

$$W = \begin{bmatrix} w_{1,1} & \cdots & w_{1,K} \\ \vdots & \ddots & \vdots \\ w_{M,1} & \cdots & w_{M,K} \end{bmatrix} \quad (39)$$

When using codebooks at both the transmitter and the receiver, the codebooks used at each end are unlikely to be the same – codebook at the receiver tends to have smaller values of  $M$ , considering aspects such as complexity, device size and price and that there is a much larger number of users. In that case, the goal is to choose a beam at the transmitter and a beam at the receiver, which together are considered an optimal beam pair, to maximise the link quality.

### 2.9.1. IEEE 802.15.3c

The IEEE 802.15.3c codebook employs only four phase shifts per element ( $0^\circ, 90^\circ, 180^\circ$  and  $270^\circ$ ) without amplitude adjustment [41]. For  $K \geq M$ , the codebook beam vectors are given by the column weight vectors of the matrix [42] - each column defines an individual beam pattern:

$$W(m, k) = j^{fix\left(\frac{m \times mod[k + (K/2), K]}{K/4}\right)} \quad \text{for } m = 0 : M - 1 \text{ and } k = 0 : K - 1 \quad (40)$$

The fix function can be substituted by the round function [42]. The former rounds each number to the nearest integer in the direction of zero and the latter rounds each number to the

nearest integer – in case of a tie, it rounds away from zero to the integer with larger magnitude. The mod function returns the remainder after division of the first input argument by the second input argument. These are MATLAB's definition of these functions.

For  $K = M/2$ , the codebook beam vectors are defined by the column weight vectors of the following matrix:

$$W(m, k) = \begin{cases} (-j)^{\text{mod}(m, k)} & m = 0: M - 1 \text{ and } k = 0 \\ (-1)^{\text{fix}\left(\frac{m \times \text{mod}[k + (K/2), K]}{K/4}\right)} & m = 0: M - 1 \text{ and } k = 1: K - 1 \end{cases} \quad (41)$$

The Array Factor (AF) of an  $M$ -element 1-D uniform-spaced antenna array generated by the  $k$ th weight vector of the codebook [43], where  $\theta$  is the polar angle in rads and  $d$  is the space between adjacent antenna elements in meters:

$$AF_k(\theta) = \sum_{m=0}^{M-1} w_m e^{jm2\pi\frac{d}{\lambda}\sin\theta} \quad (42)$$

Directivity  $D_k$  is the of gain in the direction of its maximum value relative to the gain of an ideal isotropic antenna [44]. The antenna array directivity is given by [45]:

$$D_k = \frac{\max_\theta |AF_k(\theta)|^2}{w_k^H \Omega w_k} \quad (43)$$

Where  $(\cdot)^H$  denotes the operation of Hermitian transpose,  $w_k$  is the  $k$ th weight vector in a codebook and the matrix  $\Omega$  is [45]:

$$\Omega_{n,m} = \frac{\sin 2\pi \left(\frac{d}{\lambda}\right) (n - m)}{2\pi \left(\frac{d}{\lambda}\right) (n - m)} \quad m = 0: M - 1 \text{ and } n = 1: M - 1 \quad (44)$$

This thesis explores the following combinations of  $M$  and  $K$ :

<b>M</b>	2	4		8		16	
<b>K</b>	4	4	8	8	16	16	32

Table 2-7 –  $M$  and  $K$  values evaluated in simulations

As  $M=2$   $K=4$  were the values selected for the receiver side and  $M=4$   $K=8$  the main ones for the transmitter side, only those and the ones in between them will be analysed. The polar plot of the array factors of other  $M$  and  $K$  combinations can be found on Appendix C.

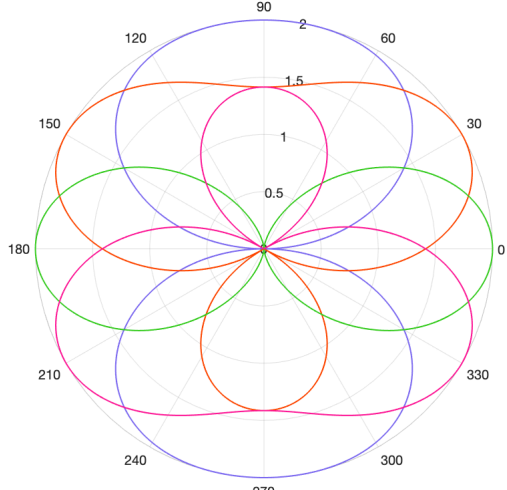


Figure 6 – 2 antenna elements, 4 beam patterns

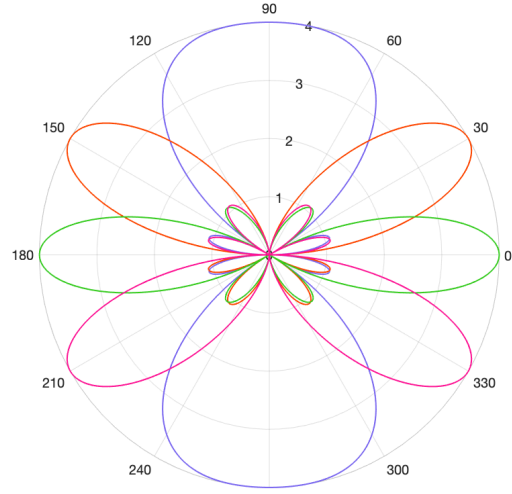


Figure 7 – 4 antenna elements, 4 beam patterns

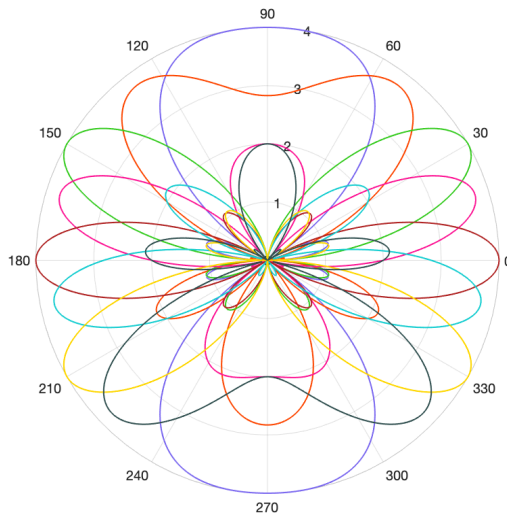


Figure 8 – 4 antenna elements, 8 beam patterns

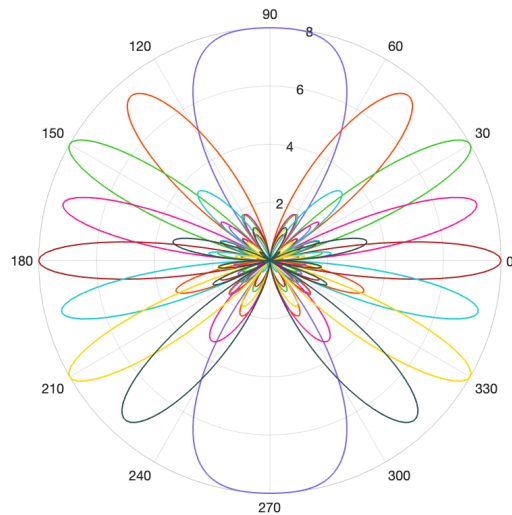


Figure 9 – 8 antenna elements, 8 beam patterns

Increasing M makes the beams narrower [7] (this can be observed in Figures 6-9), and increases the array factors and thus the antenna gains, whereas increasing K improves the angular resolution of the beams since it increases the number of beams itself. A very large K should result in many options of beams, including a beam that points exactly at the UE in the case of transmit beamforming. The BS should select the beam that points exactly towards the user as that would allow maximum gain. Although a not very large K might not result in a beam that points precisely at the UE, it can point at a considerably close angle, with almost maximum gain.

The maximum gain loss at the intersections of two beams can be reduced by setting the number of beams to twice the number of array elements [46]. According to [45], if the number of beam patterns is more than or equal to twice the number of antenna elements ( $K \geq 2M$ ), the maximum gain loss at the intersection of two beams is less than 1dB as shown on Table 2-7. This loss can be calculated as below, in dB:

$$\text{Maximum Gain Loss} = D_{max} - 10 \log_{10}(\text{intersection of beams}) \quad (45)$$

The table below shows that  $D_{max}$  (the maximum directivity) is directly related to the value of M and it does not change when the value of K is altered. More antenna elements (larger M) result in higher gain - as per [45], the maximum array gain can be calculated in dBi as:

$$\text{Maximum Array Gain} = 10 \log_{10} M \quad (46)$$

	$D_{max}$ (dB)	Intersection of beams	Gain Loss (dB)
M=2, K=4	3.01	1.848	0.343
M=4, K=4	6.02	2.612	1.85
M=4, K=8	6.02	3.343	0.779
M=8, K=8	9.03	4.71	2.30

Table 2-8: Effect of M and K on maximum directivity, intersection of beams and maximum gain loss. Calculated by the author and inspired by [45] and [44].

## Chapter 3.

### The Cellular Network Simulator

#### 3.1. Outline

A seven-cell downlink cellular network simulator was developed – where each cell has one basestation and the central cell is considered the cell of interest, being the only cell visually populated by users. To allow a thorough analysis of results, these are shown in four distinctive versions:

- i. Isotropic
- ii. Transmit beamforming: cases with different techniques for selecting beams
- iii. Transmit beamforming: modifying values of M and K
- iv. Double-directional beamforming: max-SNR and max-SINR beam selection

These versions will be explained in detail in the next chapters. The default parameters are the ones being used in the Macrocell simulation scenario. Nonetheless, parameters can be easily changed by the reader with the user interface developed by the student.

#### Network Customisable Features:

- Number of users per cell
- Number of Monte-Carlo iterations
- Radius of the hexagonal cell
- Carrier frequency
- Operating bandwidth (of a cell)
- Basestation Transmit power
- Basestation (Transmitter) antenna height
- User (Receiver) antenna height

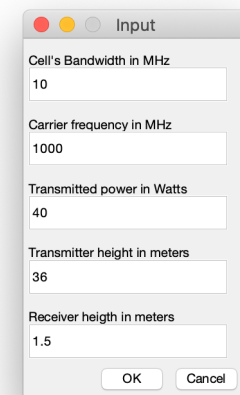
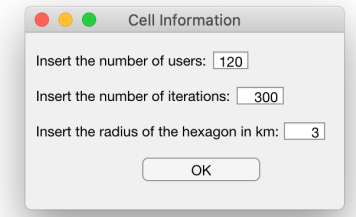


Figure 10 and 11 – Default settings (settings of the Macrocell simulation)

### Model Customisable Features:

Option of selecting one or more propagation path loss models (FSPL, Okumura-Hata, Cost-231 Hata, Cost-231 Walfisch-Ikegami, SUI and ECC-33) and their environment settings. This feature allows the comparison of the performance metrics obtained using different models – only the results of models whose boxes were ticked is displayed.

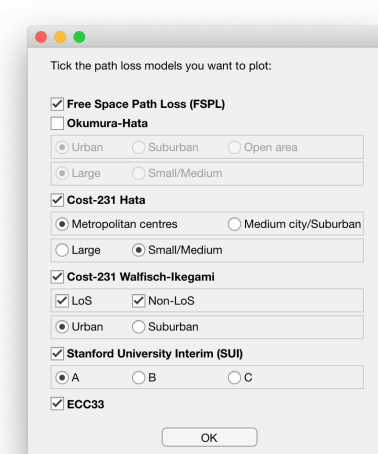


Figure 12 – Settings of the Microcell simulation (Default setting: only FSPL is ticked)

### Visual Outputs:

- Displays the seven-cell hexagonal layout with the basestations marked with '+' sign at the centre of each cell. Only the cell of interest populated with users, which are represented by '\*' (just the user coordinates from the first Monte-Carlo iteration are plotted)
- Heat Map of the seven-cell hexagonal layout in terms of the chosen performance metric
- Path losses of the selected models and their chosen environments versus the distance between transmitter and receiver
- Polar plots of the array factors of pre-determined beam patterns – the beam patterns can be plotted individually or together
- Highest array factor as a function of angle; selected beam-pattern number as a function of angle
- Statistical data plots in the form of Histograms, CDFs, and min/max/mean bar charts of the following metrics\*:
  - SNR
  - SINR
  - User Throughput
  - Cell throughput

\* of the four versions, all of which are shown in terms of the path loss model(s) chosen: i. the isotropic version (before transmit beamforming), ii. the transmit beamforming gain cases version using different strategies for picking beams and consequently, antenna gains, in a M=4 K=8 scenario, iii. the realistic uncoordinated transmit beamforming case with different numbers of antenna elements (M) and beam patterns (K) version, and iv. the double-directional final case in a Tx + Rx scenario with M=4 K=8 and M=2 K=4 for the Tx and Rx, respectively.

### 3.2. Cell Deployments

Three scenarios were simulated for this thesis, each using one of these three types of cells: macro, micro, and picocells.

Macrocell: typically used in rural areas to cover wide areas with low-density traffic [47]; macrocells require a high transmit power to maximize the covered distances, which is expensive. The antennas of the basestations are installed at a height that provides a clear view of the surroundings, so they often need to be mounted on masts, rooftops, or towers. This is the ‘regular’ type of cell, with a cell radius between 1 and 30km [48] [49].

Microcell: used in highly populated metropolitan areas, providing lower-cost commercial cellphone services. It satisfies high traffic demand in these urban areas and increases the channel capacity in smaller areas. For microcellular studies, clutter introduced by individual buildings must be accounted by the propagation models [2]. Microcells do not require a basestation as powerful and with such elevated antenna heights as macrocells do (but the transmit power and basestation antenna height of both macro and microcells are set as the same in Section 3.4 for comparative purposes), which makes microcells a more affordable option. This cell type has a radius of less than 2km.

Picocell: this cell type is often used in very high-density areas and offers very low coverage. It usually covers small indoor areas such as offices, airports, train stations, and aircrafts [50]. The transmit power requirement is considerably lower than the macrocell’s transmit power and the picocell basestation antennas are generally mounted below rooftop levels or in buildings. The maximum radius of a picocell is 0.2km.

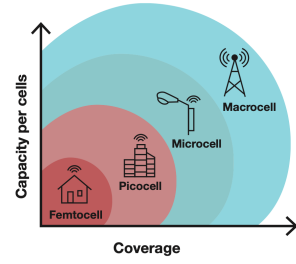


Figure 13 – Small-cell coverage.  
Source: [68]

### 3.3. Flowchart

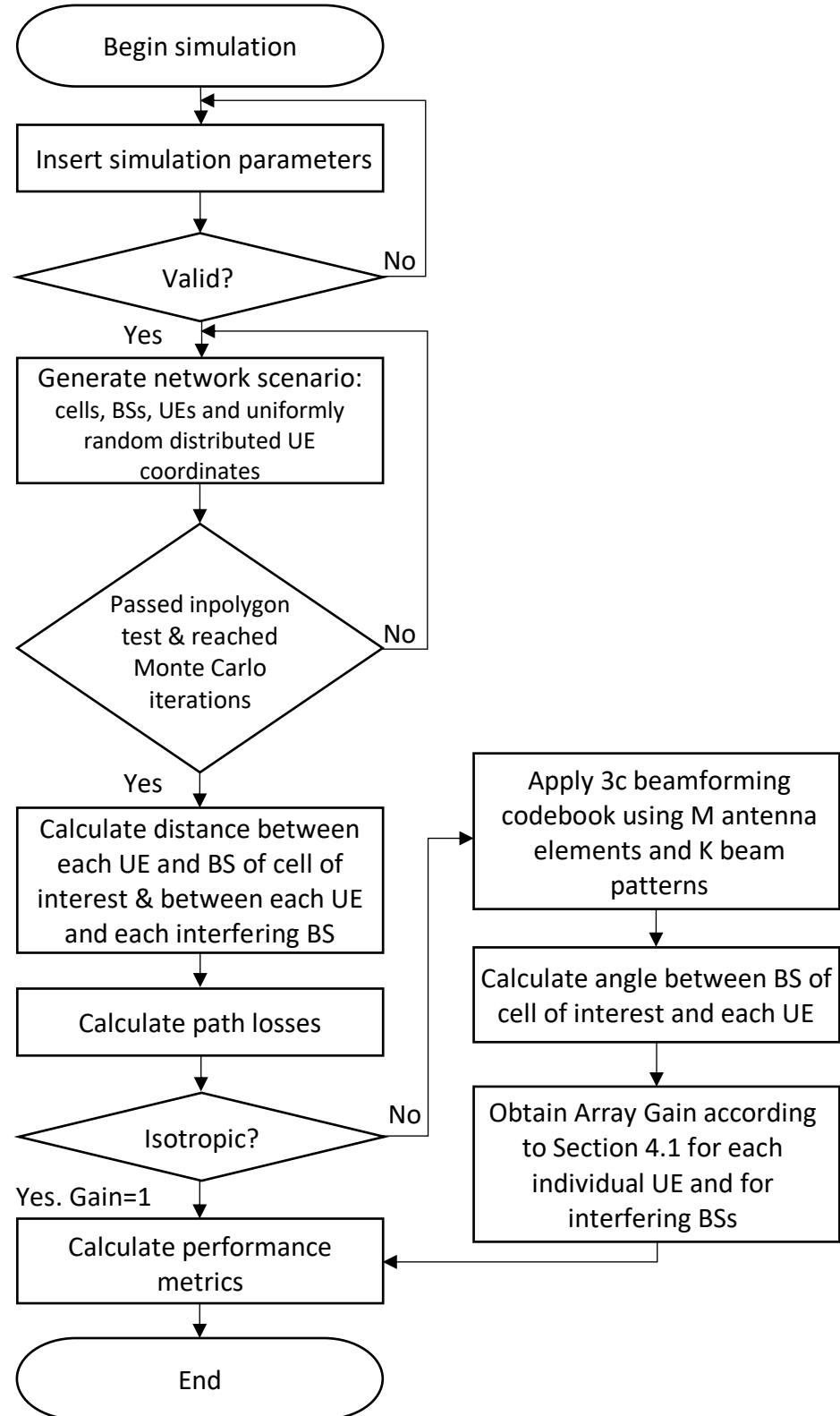


Figure 14 – Simulation Process Flow Chart. Structure inspired by [39]

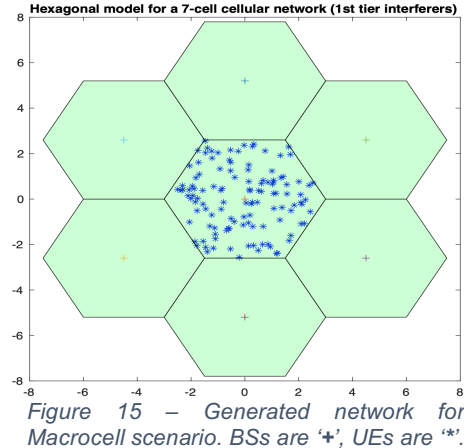
### 3.3.1. Generate network scenario: cells, BSs, UEs and uniformly random distributed UE coordinates

The BS of the cell of interest is placed at the origin and its coordinates are denoted  $C_{x_o}$  and  $C_{y_o}$ .  $R$  is the radius of the hexagonal cell and  $t$  is a vector of angles between  $0^\circ$  and  $360^\circ$ , with increments of  $60^\circ$ . To calculate the coordinates of vertices of the hexagonal cell of interest, the following equations are used:

$$x_v = C_{x_o} + R \cdot \cos t \quad (47)$$

$$y_v = C_{y_o} + R \cdot \sin t \quad (48)$$

The vertices of the interfering cells are just  $x_v$  and  $y_v$  offsetted: the vertices upper/lower cells are  $x_v; y_v \pm 2r$  and the vertices of the upper/lower right/left cells are  $x_v \pm \sqrt{3}r; y_v \pm r$ . Similarly, the coordinates of the BSs of the interfering cells are stored in the vectors  $C_{x_i}$  and  $C_{y_i}$  and are obtained by offsetting  $C_{x_o}$  and  $C_{y_o}$ : BS coordinates of upper/lower cells are  $C_{x_o}; C_{y_o} \pm 2r$  and the vertices of the upper/lower right/left cells are  $C_{x_o} \pm \sqrt{3}r; C_{y_o} \pm r$ .



The coordinates of the uniformly random distributed users of the cell of interest are obtained using:

$$xqtrial_{i,:} = C_{x_o} + R - (R + R) * rand(1, U) \quad (49)$$

$$yqtrial_{i,:} = C_{y_o} + r - (r + r) * rand(1, U) \quad (50)$$

Where  $r$  is the apothem (centre to mid-point of a side) of the hexagonal cell and it is also the extreme height of the hexagonal cell,  $i$  is the Monte Carlo iteration number of the for loop and  $rand$  is a MATLAB function that generates a 1-by- $U$  matrix of uniformly distributed random numbers between 0 and 1. These equations were developed considering that  $U$  random numbers in the interval  $(a, b)$  can be generated with the formula  $a + (b - a) * rand(1, U)$ . For  $xqtrial$ , the interval is  $(-R, R)$  and for  $yqtrial$  it is  $(-r, r)$ . It is worth highlighting that, in reality, user positions can change at any time, so this is just a representation of their coordinates at a certain time. Then, the trial

coordinates ( $xqtrial$  and  $yqtrial$ ) are tested using the `inpolygon` MATLAB function that returns ‘in’ indicating whether the query points specified by  $xqtrial$  and  $yqtrial$  are inside of the polygon area defined by  $x_v$  and  $y_v$ . If the coordinates did not pass the test a while loop inside the U (number of users) and Iter (number of Monte Carlo iterations) for loops is entered and these coordinates are replaced by a new ones, which are then tested with `inpolygon` again— this while loop is only exited once the coordinates pass the `inpolygon` test. This ensures all users coordinates are inside the hexagonal cell of interest.

The  $xqlin$  and  $yqlin$  vectors store the user coordinates from now on – they are just 1-by-U\_store vectors, which facilitate the logic of further calculations involving coordinates of six basestations as it is more convenient to keep variables to a matrix indexing to a 2 subscript level (e.g.: indexing of distances between each of the 6 interfering BSs and each of the U\_store users is much simpler than the distance between each of the 6 interfering BSs and each of the U users in each Iter iteration). U\_store is the total number of repetitions: the number of users U multiplied by the number of Monte Carlo iterations Iter.

### 3.3.2. Calculate distance between each UE and BS of cell of interest & between each UE and each interfering BS

The Euclidean distance is calculated using the “distanceangle” function written by the author. The Euclidean distance is calculated as per the formula below:

$$d(BS, UE) = \sqrt{(x_{UE} - x_{BS})^2 + (y_{UE} - y_{BS})^2} \quad (51)$$

For the calculation of the distance between each UE and the BS of the cell of interest, it is essentially calculating the distance between the origin (central BS coordinates) and each UE, stored in a 1-by-U\_store matrix. The same formula is used to calculate the distance between each UE and the interfering BSs, but it results in a matrix of 6-by-U\_store.

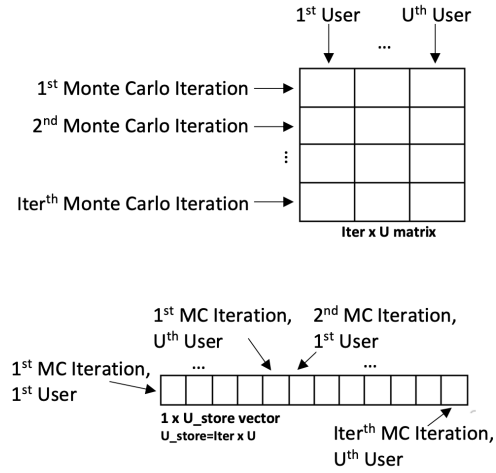


Figure 16 – Illustration of the change from  $xqtrial$  and  $yqtrial$  matrices to  $xqlin$  and  $yqlin$  vectors.

### 3.3.3. Calculate path losses

The path losses of each model are calculated as described in Section 2.8 – the distances obtained in Section 3.3.2 are required. Each propagation path loss model has its own function and the environments are selected using the “checkboxPLmodels” function (as seen in Figure 12) that also determines which propagation path loss models results will be plotted.

### 3.3.4. Calculate angles between BS of cell of interest and each UE

The angles of departure (between BS and UE) and of arrival (between UE and BS) are also calculated using the “distanceangle”:

$$\text{angledeparture} = \text{atand} \left( \frac{y_{BS} - y_{UE}}{x_{BS} - x_{UE}} \right) \quad (52)$$

$$\text{anglearrival} = \begin{cases} \text{angledeparture} + 180^\circ & \text{for } \text{departureangle} < 180^\circ \\ \text{angledeparture} - 180^\circ & \text{for } \text{departureangle} > 180^\circ \end{cases} \quad (53)$$

Where atand is the MATLAB in-built function that returns the inverse tangent in degrees. The central angles of departure and of arrival, angledep\_centeralBSUE and anglearriv\_centeralBSUE, are calculated as well as the interfering angles of departure and of arrival, angledep\_interfBSUE and anglearriv\_interfBSUE.

### 3.3.5. Apply 3c beamforming codebook using M antenna elements and K beam patterns / Obtain Array Gain for each individual UE and Array Gain of interfering BSs

The “beamforming3c720” function created by the author takes the frequency, the angle of departure (for Tx beamforming) or of arrival (for Rx beamforming), the number of antenna elements M, and the number of beam patterns K. The interfering antenna gains are obtained using angledep\_interBSUE or anglearriv\_interBSUE and the central antenna gains are obtained with angledep\_centeralBSUE or anglearriv\_centeralBSUE – this process is completed for each user and each basestation: the results for different basestations obtained using the same user are stored in different rows and the results for different users using the same basestation are stored in different columns, in a matrix of 1-by-U\_store size for the central BS inputs and of 6-by-U\_store size for the interfering BSs inputs. This function has the antenna element spacing is set to  $\lambda/2$  as discussed in Section 2.9

and generates 3c codebook column weight vectors (codebook matrices) according to Section 2.9, as well as the Array Factors and directivity.

The Array Factor is a K-by-721 matrix. There are 721 angles, with a  $0.5^\circ$  precision (e.g.: angle 1 is  $0^\circ$ , angle 2 is  $0.5^\circ$ , angle 5 is  $2^\circ$ , angle 721 is  $360^\circ$ , and so on). The input angle (angle of departure for transmit beamforming or angle of arrival for receive beamforming) is multiplied by 2, rounded down using MATLAB's floor function and this resulting angle needs to be incremented by 1 so that the result matches one of the 721 angles.

For example, if the input angle is  $247.7258^\circ$ , it is multiplied by 2 (becomes  $49.4515^\circ$ ), rounded down to  $49^\circ$  and its array factor (linear antenna gain) is going to be on the 50<sup>th</sup> column of the Array Factor so the angle has to be incremented by 1 after being rounded down (MATLAB indexes start at 1, so  $0^\circ$  is placed at the 1<sup>st</sup> index). On this column, of the K beams (rows) is selected according to the goal (maximum/minimum/random gain), returning the beam index selected and the resulting gain. The concepts of maximum, minimum and random will be explained later.

### ***3.3.6. Calculate Prx, SNR, Interference, Bandwidth Efficiency, User Throughput, Cell Throughput***

The antenna gain value from 3.3.5 needs to be converted to dBi to calculate the wanted (using the PL calculated with the distance between UE and central BS) and interfering received powers (using the PL calculated with the distance between UE and interfering BSs), all of which are accomplished by the function named “linkbudget” – the sum interfering received power is exclusively calculated using the “sumInter” function that calls “linkbudget”. After, the performance metrics are calculated as described in Chapter 2. The goal of the antenna gains can vary according to the beam selection of the cases that will be introduced in Chapter 4, and if Isotropic the antenna gain is 1 (0 dBi). The results of each metric are stored in matrices: each row represents the result obtained with the path loss propagation model number. (1=FSPL, 2=Okumura-Hata, 3=Cost-231 Hata, 4=LOS Cost231-Walfish-Ikegami, 5=Non-LOS Cost231-Walfish-Ikegami, 6=SUI, 7=ECC33).

There is a limit to the maximum values of SINR, user and cell throughputs – this is displayed in Table 3-1. The existing modulation schemes have bandwidth efficiency limits, this consequently sets a limit to SINR and to user and cell throughputs. The cell throughput limit is only reached if all

the users reach the user throughput boundary. Therefore, this will not be visible in this thesis as there is no scenario simulated in which the user throughputs of all users reach the limit. The modulation scheme 256 QAM (Quadrature Amplitude Modulation) is one of the schemes with highest theoretical bandwidth efficiency limits [51]: 8 bits/sec/Hz [52], so 30dB as an SINR hard limit is a good approximation as the maximum bandwidth efficiency of this thesis was set as 9.9672 bits/sec/Hz.

### 3.4. Monte Carlo passes

The number of Monte Carlo iterations makes a significant difference on the results, especially when it comes to cell throughput. The larger the number of Monte Carlo passes, the smoother the curves are and the more accurate the results, but this comes at a cost of simulation time. 300 Monte Carlo cells for 120 users is a good trade-off, as the CDF curves were not much smoother with 600 iterations in Figure 17 and would require more simulation time. However, for fewer users, more Monte Carlo passes would be needed to provide the same type of accuracy – it all depends on U\_store, the multiplication of number users and number of Monte Carlo passes.

The results presented in this thesis have a U\_store of 36000 (120 Users, 300 Monte Carlo Iterations). 300 Users and 120 Monte Carlo Iterations would result in the same smoothness for SNR, SINR, and User throughput, but not for Cell throughput as there would only be 120 Cell throughput values since cell throughput is the sum of user throughput of all users in a cell.

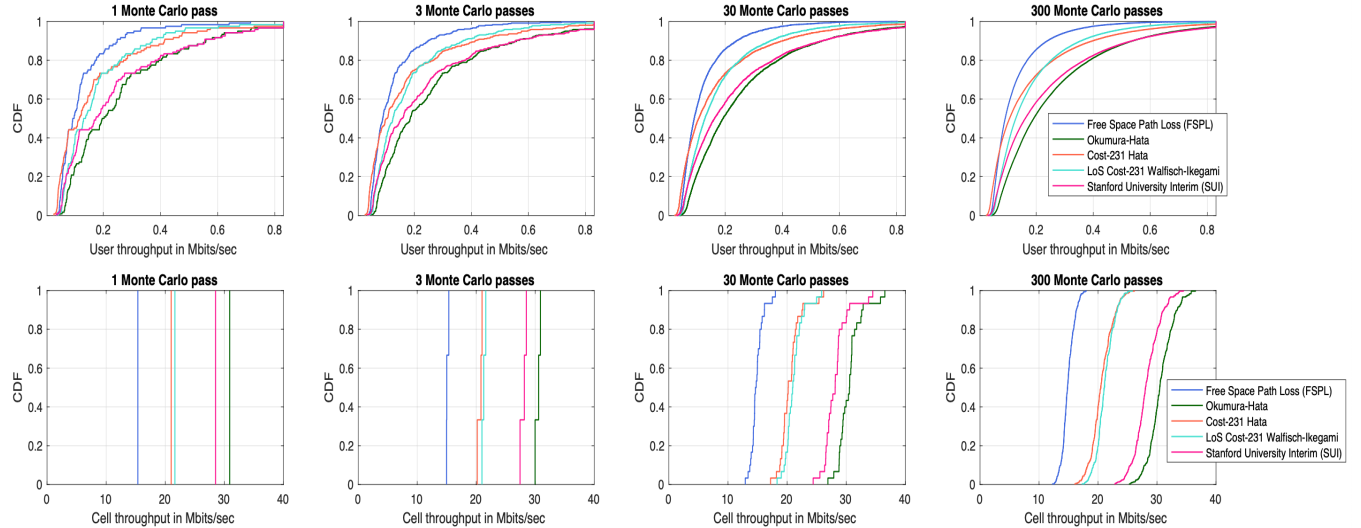


*Figure 17 – The impact of the number of Monte Carlo passes on the Cumulative Density Function (CDF) curves of the user and cell throughputs.*

### 3.5. List of Assumptions

Parameter	Macro-cell	Micro-cell	mmWave Pico-cell
Cell Layout	Seven-cell hexagon layout		
Operating Bandwidth	10MHz	100MHz	1000MHz or 1GHz
Cell Radius	3km [53]	0.5km	0.1km
Total Simulation Area	163.681km <sup>2</sup>	4.5465km <sup>2</sup>	0.7274km <sup>2</sup>
Cell simulation Area	23.383km <sup>2</sup>	0.6495km <sup>2</sup>	0.1039km <sup>2</sup>
Carrier Frequency	1000MHz or 1GHz	3500MHz or 3.5GHz	28000MHz or 28GHz
Frequency Reuse Strategy	Cluster size = 1		
Transmit Direction	Downlink (from BS to UE)		
Base stations	Basestation Transmit Power		46dBm (40W) [54]
Base stations	Basestation Height		36m [55]
Base stations	Antenna Radiation Pattern		
Users	Number of Users (Central Cell)		
Users	0.0833MHz	0.833MHz	8.33MHz
Users	User Coordinate Distribution		
Path loss	User Height		
Path loss	Noise Model		
Path loss	Noise Figure NF		
Path loss	Interference Model		
Model settings	Noise	-93.98dBm	-83.98dBm
Model settings	1. FSPL	✓	✓
Model settings	2. Okumura-Hata	✓ Open area; Large	✗ Up to 1500MHz
Model settings	3. Cost-231 Hata	✓ Medium city/Suburban; Large	✓ Metropolitan centres; Small/medium
Model settings	4. LoS Cost-231 Walfish-Ikegami	✓	✗
Model settings	5. Non-LoS Cost-231 Walfish-Ikegami	✗ Unfeasible for rural areas	✓ Urban; Building separation=50m; Angle=30°
Model settings	6. SUI	✓ Type C [32]; s=8.2	✓ Type A [32]; s=10.6
Model settings	7. ECC33	✗ Unfeasible for rural areas [32]	✓ Type A; s= 10.8; $\alpha_{NLOS} = 0.71$
Simulation	Bandwidth Efficiency Limit	9.9672 bits/s/Hz	
Simulation	SINR Limit	30dB [56] [51]	
Simulation	Monte Carlo	300 passes	

Table 3-1 – List of Assumptions

### 3.6. Macrocell Simulation Scenario

The numerical results obtained and trends of Figure 19 are closely related to those in [25] and [57] as the parameters are very similar, validating this simulation. As mentioned in [57], Cost-231 Walfisch-Ikegami does not have an appropriate setting for rural environments, so LoS Cost-231 Walfisch-Ikegami is used in these situations – the LoS does not respond to changes on the antenna's heights as building obstructions are not considered in its equations.

Similarly to [25], Okumura-Hata overcomes FSPL at approximately 0.4km separation distance. When analysing the FSPL and LoS Cost-231 Walfisch-Ikegami formulas, it is possible to state that the path loss difference between these two models is always equivalent to  $6\log_{10} d + 10.15$  and therefore the disagreement between them increases with distance, as evidenced in Figure 19.

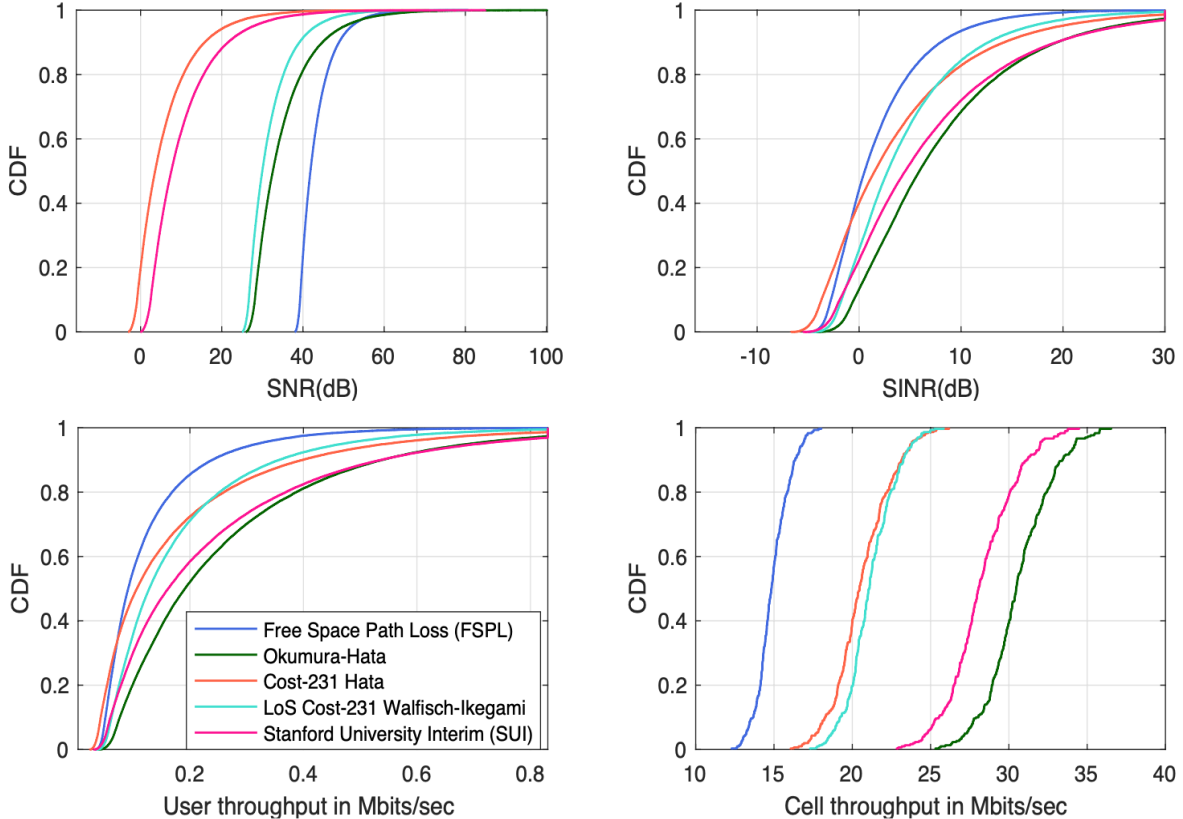


Figure 19 – Performance metrics using the valid Propagation Path Loss Models for the Macrocell scenario.

Cost-231 Hata is an extension of the Okumura-Hata model for frequencies that exceed Okumura's range (maximum valid carrier frequency is 1500MHz), but this is not the case of this simulation scenario since the carrier frequency being used is 1000MHz. Therefore, further investigation should be carried using the Okumura-Hata model for the Macrocell simulation – this can be found on Appendix A.

Additionally, it is worth mentioning that Okumura-Hata's user throughput CDFs indicated the highest probability of getting a high user throughput (the curve starts further to the right) compared to the CDFs of other models, which is desirable. This can then be confirmed when analysing the cell throughput in Figure 19: Okumura-Hata has the largest cell throughput when compared to the other valid path loss models.

From the Link Budget equation (11), the received power of an isotropic analysis is inversely proportional to the path loss. This behaviour can be observed on the SNR graph, as changes in SNR depend on the value of the received power (noise is constant as the bandwidth, temperature and figure of noise are the same for all models in a simulation scenario). FSPL has the highest SNR as it has the least significant path loss.

### 3.7. Microcell Simulation Scenario

The path loss results obtained are extremely similar to those in Figure 4.1 of [58] with few discrepancies in terms of value, thus validating the simulations performed by the author. These inconsistencies due to the receiver's antenna height and to the fact that the paper uses SUI type "C", whereas "A" is being used to represent urban environments in this dissertation – the SUI's behaviour should be compared to that of [59], as both of them use the same SUI environment. It can be observed that SUI overtakes FSPL's curve at 0.35km, in accordance with [59].

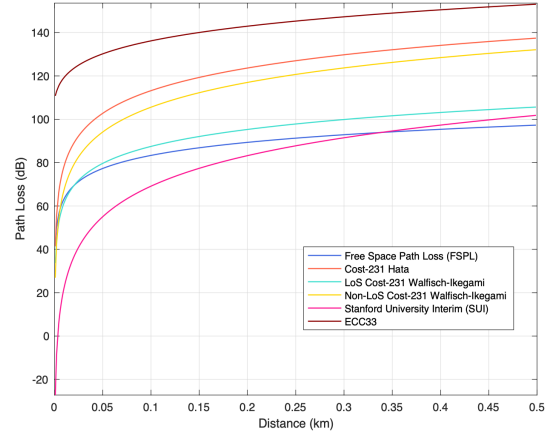


Figure 20 – Path Loss versus Distance for valid Propagation Path Loss Models.

As proven in [58] and [59], the ECC-33 model is highly impacted by changes in the receiver's antenna height and it overestimates the path loss at low receiver's antenna heights – Figure 19 shows how this exaggerated path loss can influence the performance metrics as there is a significant difference between ECC's metrics and the metrics from other models.

The SUI model offers minimum path loss in this case, however, it might not be the most realistic option when considering the parameters being used as it can be too optimistic (it is SUI's type A)– further analysis should be carried using the Non-LoS Cost-231 Walfisch-Ikegami model as it is the preferred option when studying microcell in small urban environments. Cost-231 Walfisch-Ikegami takes more environment information into account than Cost-231 Hata does [60], such as orientation angle, building distance, and rooftop heights. Hence, as semi-deterministic model, Cost-231 Walfisch-Ikegami tends to have better accuracy than empirical models.

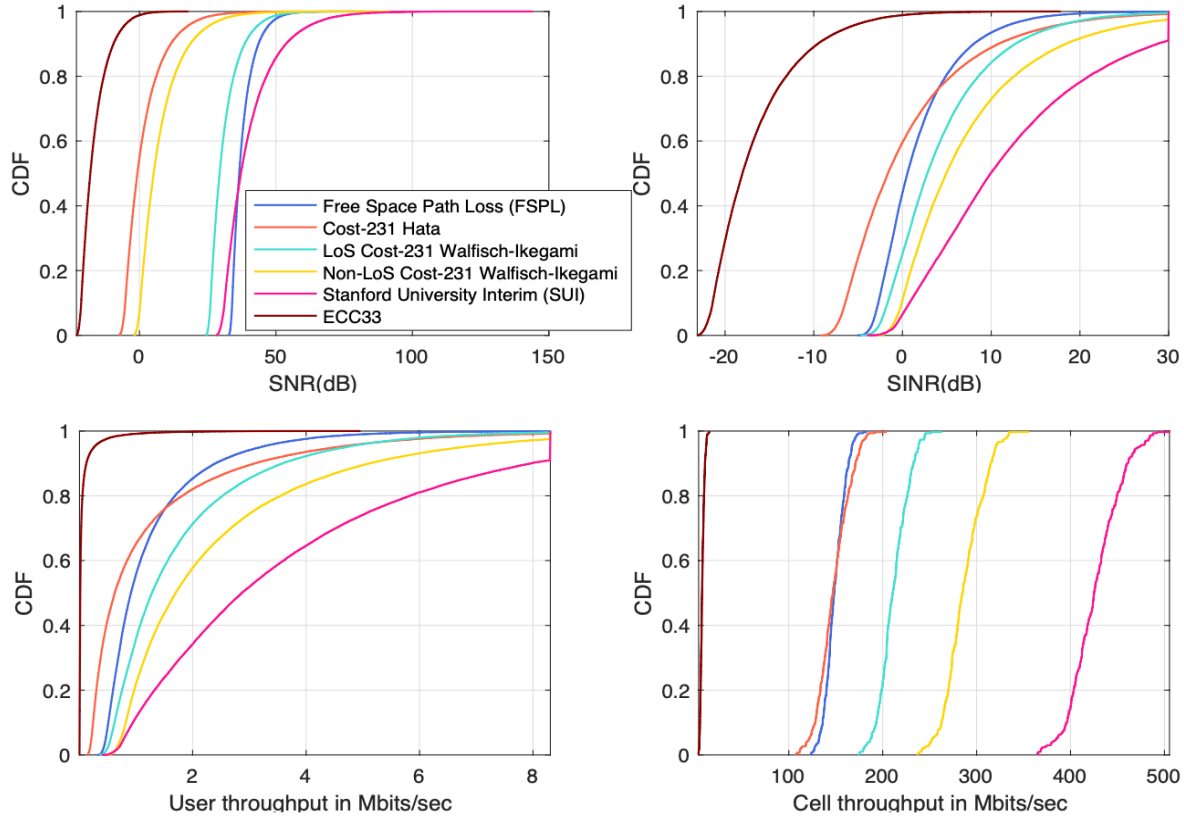


Figure 21 – Performance metrics using the valid Propagation Path Loss Models for the Microcell scenario settings.

It is worth emphasizing that the maximum user throughput is 8.3Mbits/sec for the Microcell simulation scenario and 0.83Mbits/sec for the Macrocell simulation scenario. The explanation for that is in Table 3-1, as the operating bandwidth and user bandwidth of the Microcell are 10 times the

values set for the Macrocell. The user throughput depends largely on the bandwidth efficiency and, consequently, on the SINR, which are kept to 9.9672 bits/s/Hz and 30dB, respectively. The change in cell size (from Macro to Micro) is also partially accountable for the increase in cell throughput [51].

### 3.8. mmWave Picocell Simulation Scenario

As only two path loss models (modified SUI and FSPL) were valid for the mmWave Picocell simulation scenario, there is no need to make a comparison between path loss models and, understandably, modified SUI is the selected for further analysis of this scenario.

The main restriction in terms of model parameters for this scenario is related to the mmWave frequency – all of the other Path Loss Models implemented on this project were not valid for such frequency range. Modified SUI's path loss is lower than FSPL's, as the modified FSPL model from [34] was not been implemented to the software created for this thesis. The SUI's isotropic performance metrics will be available in the next chapters. This simulation scenario is studied further in Chapters 4, 5, and 6.

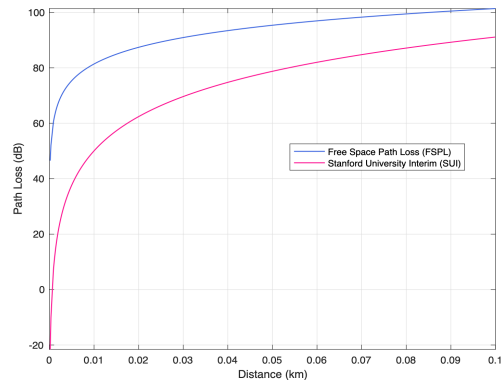


Figure 22 –mmWave Picocell Scenario: Path Loss versus Distance for valid Propagation Path Loss Models.

## Chapter 4.

### Transmit Beamforming

In this chapter, transmit beamforming using the IEEE 802.15.3c codebook will be studied to achieve a trade-off between minimum interference and maximum gain [39]. The selection of beam patterns will be based on the antenna gain according to the cases presented in Section 4.1, which are simulated using  $M=4$  and  $K=8$ , as illustrated in Figure 23, and applying mmWave Picocell parameters with SUI model type A. Considering that multiple antennas are being used in the array of antennas of the transmitter, there is a “Multiple Input” and as the receiver only uses one isotropic antenna, it is “Single Output”, thus making it a “Multiple Input Single Output” (MISO) system.

The type of beamforming taxonomy that fits best the beamforming strategy used in this thesis is the switched beamforming defined in [61], as it refers to pre-determined (requires codebook) beam patterns with different amplitudes and phases that cover the azimuth angles of  $360^\circ$ . The transmitter (BS) chooses the beam that sends the strongest signal (main lobe), which is the beam that points at the direction of the user determined by its angle of arrival. However, unlike what is stated in [61], beamforming in this project uses minimal channel information and is a much more sophisticated approach.

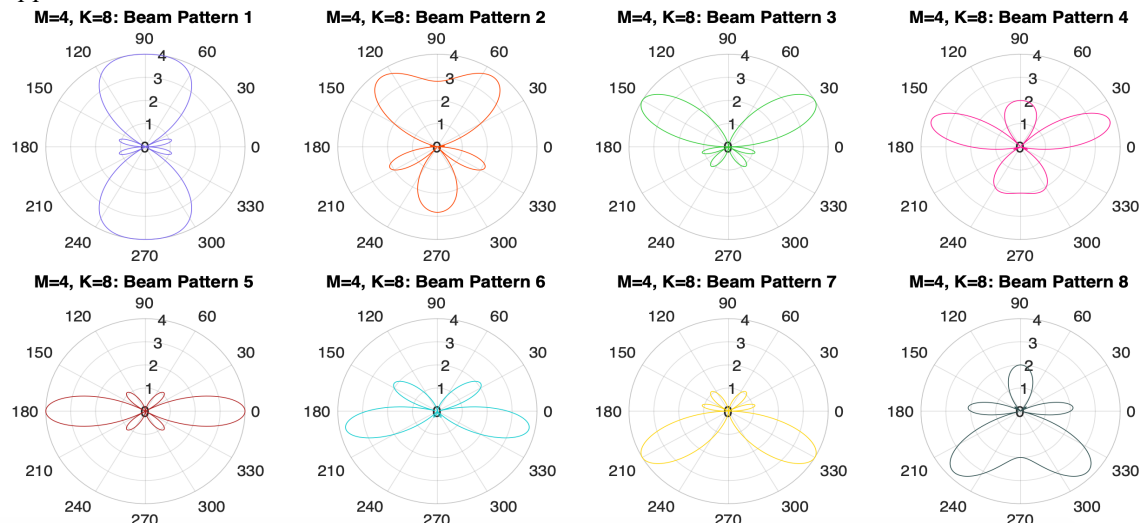


Figure 24 – 8 beam patterns generated by an antenna array of 4 antenna elements. Each polar plot shows the main lobes and side lobes of a beam pattern. E.g.: For a user with an angle of departure of  $31^\circ$ , the BS best beam (results in highest gain) is 3 and the BS worst beam (lowest gain) is 8. For a user with an angle of departure of  $110.5^\circ$ , the BS best beam is 1 and the worst is 6.

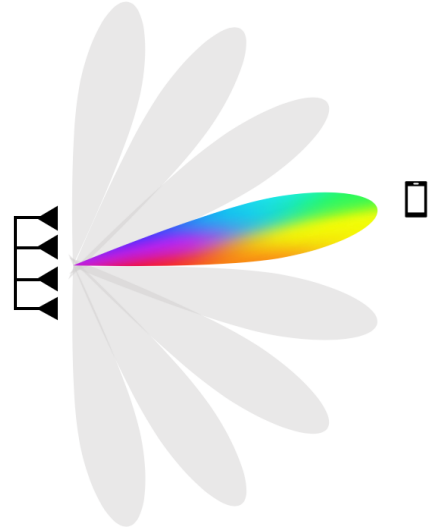


Figure 23 – Downlink MISO using antenna array of 4 antenna elements to generate 8 beam patterns. Only main lobes were illustrated. Image created by the author, inspired by [69].

## 4.1. Transmit Beamforming Cases

There are many approaches that basestations can use to choose beams for their users. The methods being evaluated here, denoted as cases, consist on just a few of the existing possible ways of selecting beams. The selection processes described in the cases occur for each basestation selecting a beam for a particular user.

### Isotropic

The antenna emits radiation equally in all directions. It is the case used in Chapter 3, in which the antenna gain on both sides is always 1 (0dBi) [2]. Isotropic results are used as a ‘reference’ to the cases of this chapter, showing whether the case improves or impairs the performance metrics when compared to this reference.

### Case A: Upper Bound Transmit Beamforming

This case represents the idea that the basestation of every cell is trying to look after the users of the cell of interest instead of looking after its own users. This idea is considered idealistic, providing an unrealistic combination that results in maximum SINR (maximum received power, minimum interference) and thus should only be used to quantify an upper limit on the expected benefits.

Every interfering basestation picks the beam that result in the lowest gain (worst for its own users, best for the users of the cell of interest), providing minimum interference to the cell of interest. The central basestation chooses a beam for each user so that the antenna gain is maximum, improving the SNR.

### Case B: Random Beam Selection

The central basestation randomly chooses a beam for each user. The same applies occurs to the interfering basestations: each of these basestations selects a random beam for each of the users located at the central cell. Inevitably, all gains in this case are random. The results are expected to be inferior to the Isotropic ones.

### **Case C: Uncoordinated Beamforming**

In each cell, the basestation is trying to look after its users. Every interfering BS selects a beam such there is maximum gain (best for its own users, worst for the users of the cell of interest), maximising the interference as a consequence. Similarly, the central BS picks the beam that provides maximum gain for each UE, improving SNR.

This case cannot be considered realistic since the cochannel cells were not populated during the simulation and it cannot truthfully represent idea that every BS is looking after its own users by simply selecting the beams that have the highest gains as the interfering cells have no users to consider the direction (angle of departure between interfering BS and one of its UEs). These cochannel BSs are just selecting the beam whichever delivers the highest gain, but the beams available were generated according to the angle of departure between interfering BSs and central UEs. The best gain for the unpopulated interfering cells might not be the best gain for its UEs if these interfering cells were populated. This should not necessarily improve the SINR.

### **Case D: Realistic Uncoordinated Beamforming**

This case is intended to be an improved version of Case C. The central BS selects a beam for each of the UEs according to the gain, so that the gain is maximised. Unlike Case C, this case considers that the user distribution of the cochannel cells should not be the same as the user distribution of the cell of interest, so the angles between interfering BSs and their own UEs are unlikely to be the same.

Just like in the previous cases, the interfering BSs are still using the angles of departure between interfering BSs and central cell UEs for beam-selection purposes. The difference is that these cochannel BSs are ‘randomly’ picking the beams so that the principle of “each basestation is trying to look after its own users” is applied. In reality, the interfering beams are not truly being chosen randomly: the interfering BSs selection of beams for each of its own UEs is seen as random from a central cell point of view. The beam selection occurring for a certain interfering BS for each of its users is uncorrelated to the central BS selection. Thus, Case D is considered a realistic representation of uncoordinated beamforming.

## 4.2. Results

As previously mentioned in Section 2.9, codebook-based Tx beamforming is considered particularly attractive for mmWave frequencies because it alleviates the extremely high path losses from these frequencies. Therefore, the analysis is conducted using the simulation scenario with such frequencies to confirm this hypothesis.

All Cases - with exception of Case B, in which the central BS randomly selects a beams for each of the users of the central cell – have exactly the same SNR values as seen in Figure 25 and presented a increase of 24.6% in comparison with the average Isotropic SNR. The reason for that is that in these cases the central BS chooses the beam that delivers the highest antenna gain for each user, so they all have identical received powers.

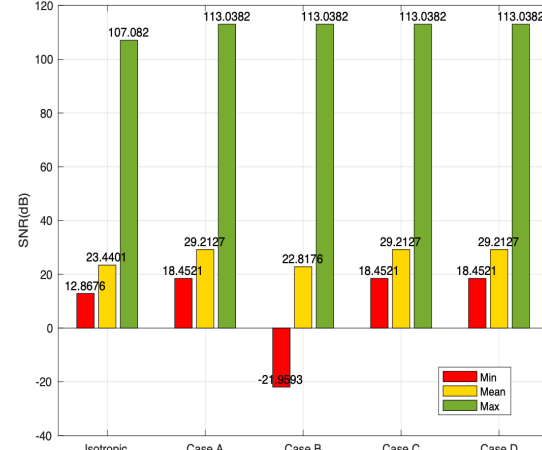


Figure 25 – mmWave Picocell, SUI model: Minimum, mean and maximum SNR

As Figure 26 shows, the minimum value of SINR dramatically decreased by 938.3% when comparing Case B to Isotropic – this rate can vary slightly every time as new random beams are selected in each simulation. As Case B is a random case, the severity obviously cannot be predicted, but it always presents a disadvantage for users, particularly for those at cell-edge. Case A presents an overly-optimistic increase for users at the cell-edge, with the minimum value of SINR being boosted by 233.1%. This is the first indicator that Case D is the most realistic case, increasing cell-edge users SINR by 6.5%.

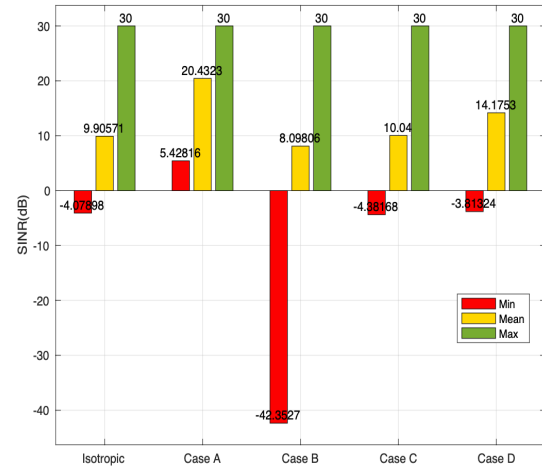


Figure 26 – mmWave Picocell, SUI model: Minimum, mean, and maximum SINR.

Case C, as expected, did not present significant improvement for any of the metrics that consider interference. This suggests that the gain from beamforming of the interfering BSs, which adds to interference, is so high that it cancels out the improvements from central BS beamforming that was added to the received power. Case D is the realistic uncoordinated case that consistently lies between Case C and Case A, providing a more faithful estimate of what uncoordinated transmit beamforming using M=4 and K=8 achieves.

The hard limits of bandwidth efficiency and consequently of SINR are noticeable in Figure 27. This limit is the cause of the CDF “leap” seen on the SINR and User throughput CDFs. When the maximum limit performance metric is achieved before the CDF reaches 1 (100%), this indicates that there might be a meaningful percentage of users achieving that upper boundary according to the length of this vertical line (leap). This percentage is particularly high for Case A as it presents the longest vertical line amongst all cases and further observed in Figure 28.

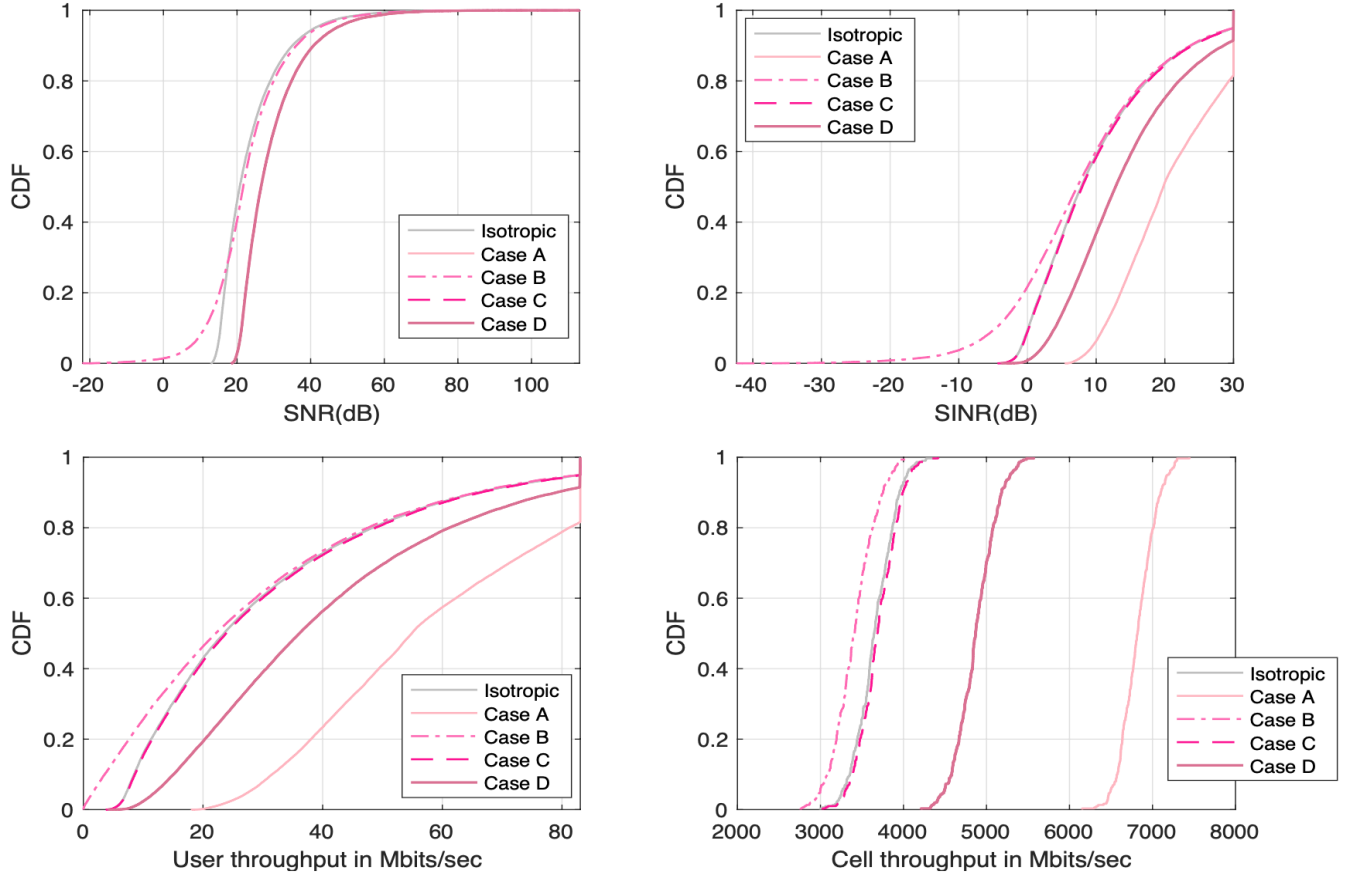
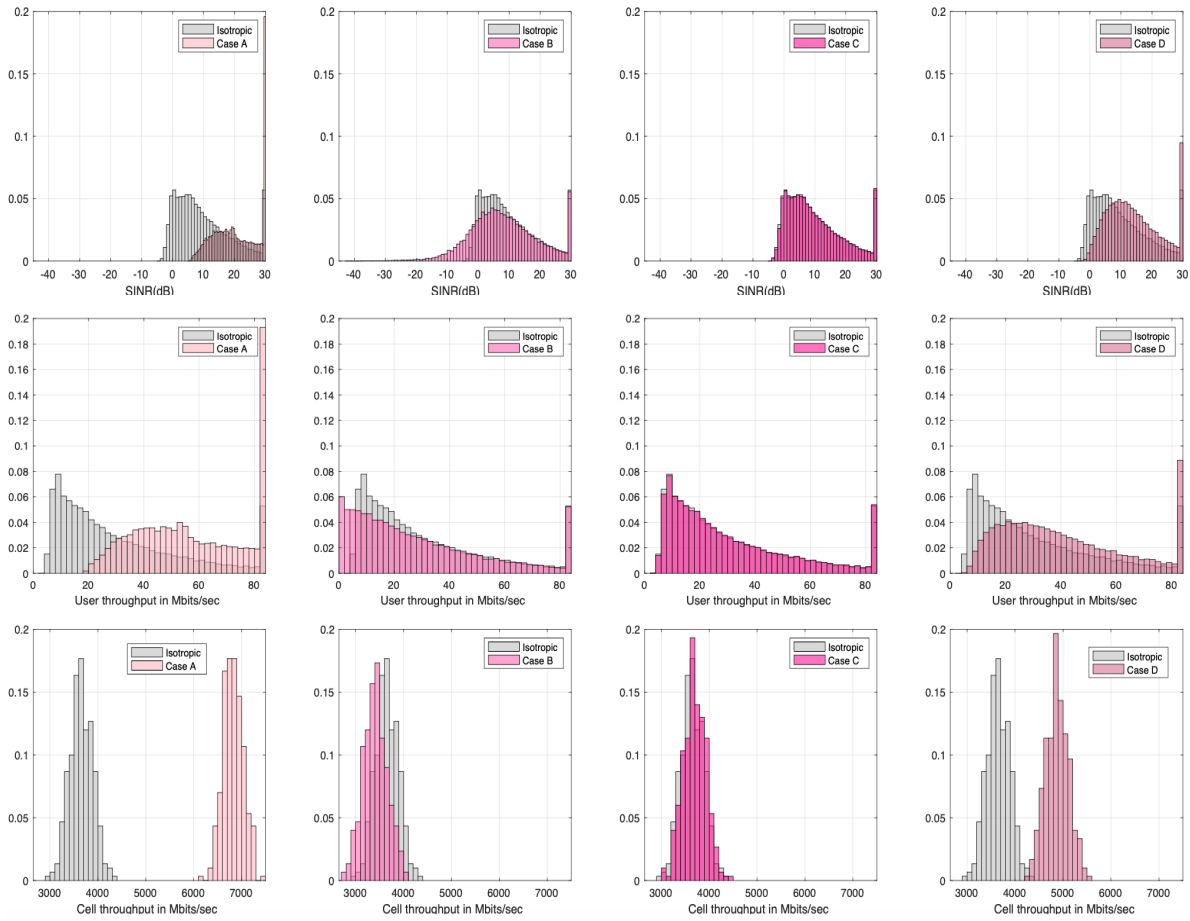


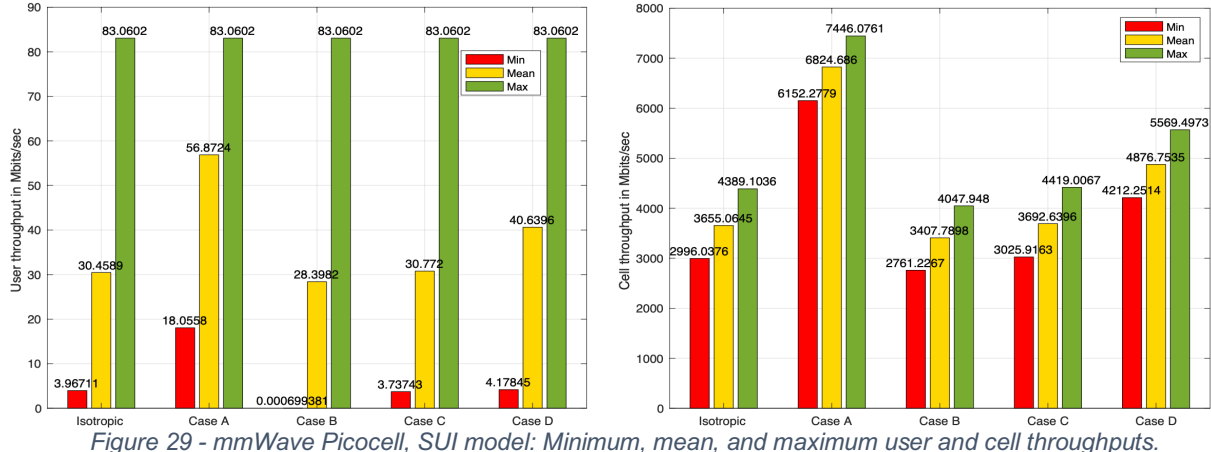
Figure 27 - mmWave Picocell, SUI model: CDF versus performance metrics, using 3c codebook beamforming at the transmit side. Different techniques for selecting the beams are applied for each case.

The histograms in Figure 28 give a more insightful visualisation of the impact of each case. Case A shifts the columns to the right by a great amount, showing enormous overall improvement for all users. Case B shows an overall deterioration. Case C shows the worsening of metrics for users at the cell edge whilst slightly enhancing the metrics for users at the cell centre, consequently having little improvement overall. Even though Case D does not enhance the performance as much as A does, it still offers a meaningful enhancement for all users in all metrics, thus fulfilling the purpose of transmit beamforming.



*Figure 28 - mmWave Picocell parameters, SUI model: Histograms. Frequency (percentage) of occurrence versus performance metrics.*

As calculated from Figure 29, both average user and cell throughput had an overall increase of 86.7% with Case A, an overall decrease of 6.8% with Case B, an overall increase of 1.05% with Case C, and an overall increase of 33.4% with Case D. Similar trends were observed when analysing Microcell Simulation and Microcell Simulation results – these can be found on Appendices A and B.



### 4.3. Conclusion

As evidenced in this chapter, the benefits of transmit beamforming are irrefutable for Cases A and D. Case A delivered the best results, however, it relies on principles that relate to coordinated beamforming. This refers to coordinating the resource allocation according to a certain resource that is being shared in a communications channel (e.g.: FDMA, CDMA), which requires inter-cell communication. In other words, the BS of every cell is looking after its own users, but these users are grouped in a way that they interfere as little as possible with each other. This concept is explored in [62] and [63]. The latter examines altruistic and egoistic approaches of coordinated beamforming.

Case A is very optimistic and unachievable even in terms of coordinated beamforming, as it focuses only on what is best for the central cell. In reality, coordinated beamforming would attempt to coordinate to benefit every cell instead of benefiting only the central cell. This leads to the conclusion that applying coordinated beamforming or selected coordinated beamforming could be beneficial and that the performance metrics would show significant improvement, but not to the extent of achieving results as high as Case A's.

Despite the fact that Case D results slightly vary each time interfering BSs beamforming occurs due to new sets of random beam pattern indexes being chosen, the deviation in overall results is not tremendously significant (usually less than 3%) and it still always leaves Case D positioned between Case C and A. Its randomness is what makes it realistic: the beams selected by interfering BSs for each of its users is seen as random from central cell perspective. As it is the most realistic case for uncoordinated beamforming presented and it has been proven to be effective in terms of enhancing the results for users at the cell-edge, Case D will be further analysed in Chapters 5 and 6.

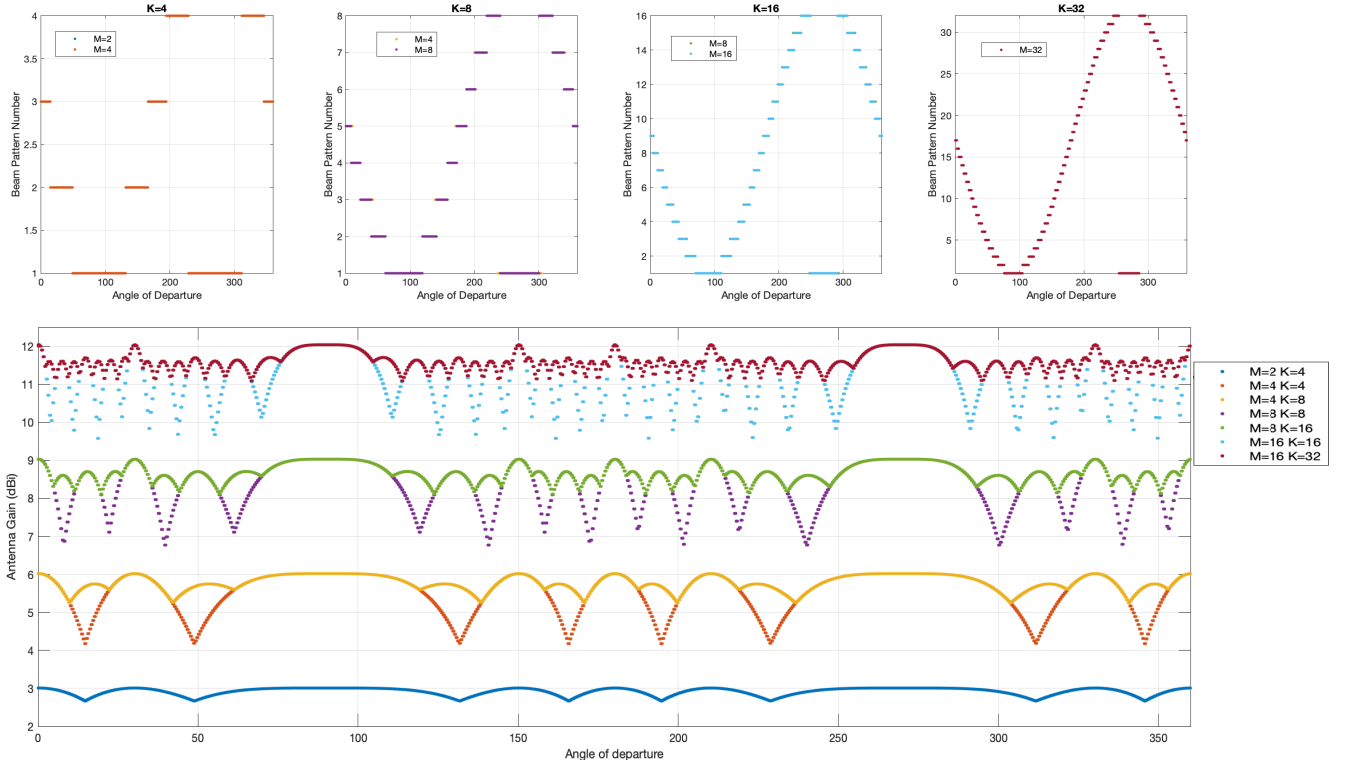
## Chapter 5.

### The Impact of Basestation Antenna Configurations on Transmit Beamforming

This chapter focuses on exploring the benefits of varying the values of M and K for transmit beamforming only, which were briefly reviewed in Section 2.9. mmWave frequencies facilitate the use of larger antenna arrays [5] – very high frequencies reduce the physical size of the directional antennas and the wavelength, consequently decreasing the uniform spacing as it is set to  $\lambda/2$  [64]. In this study, M varies from 2 to 16, and K varies from 4 to 32, allowing both K=M and K=2M combinations. As previously stated, larger numbers of antenna elements (M) achieve higher maximum array gains that can be quantified in dBi as:

$$\text{Maximum Array Gain} = 10\log_{10} M \quad (54)$$

#### 5.1. Beam Pattern Selection & Highest Antenna Array Gain



Figures 30 and 31 – Beam pattern number with highest antenna gain as a function of angle of departure, grouped according to K (top). Attention: Y-axis begins at 1 and finishes at K. Highest antenna gain of central BS as a function of angle of departure (bottom).

The “constant highest antenna gain” in Figure 31 is longer for lower values of M’s and the range of angles of this constant gain matches the selection of Beam Pattern 1 in Figure 30. As M increases, the beams become narrower and this “constant highest antenna gain” remains continuous for a smaller range of angles.

K=M presents much more severe fluctuations since there are fewer options of beams to pick from and smaller probability that one of the beams available is the optimal beam pointing as precisely at the UE, thus resulting in a reduced highest (best) antenna gain at the bottom of the dips. For isotropic, the highest antenna gain would be a flat line of 0dBi regardless of the angle of departure. From (46), Maximum Array Gain obtained with twice as many antenna elements is  $10\log_{10}(2M) = 10\log_{10}(M) + 10\log_{10}(2) = 10\log_{10}(M) + 3.0103\text{dBi}$ . Considering the logarithmic properties, the maximum highest antenna gain also seems to be incremented by approximately 3.01dBi each time M doubles.

As seen in Figure 31, the highest antenna gains fluctuate considerably less for K=2M, keeping the variations (gain-loss) below 1 dB as explained in Section 2.9. K=2M has a lower maximum gain loss at the intersection of beams and has better angular resolution as there are more beams available, improving the chances of finding a beam that points almost exactly at the direction of the user, resulting in higher ‘highest antenna gains’ at the lowest points.

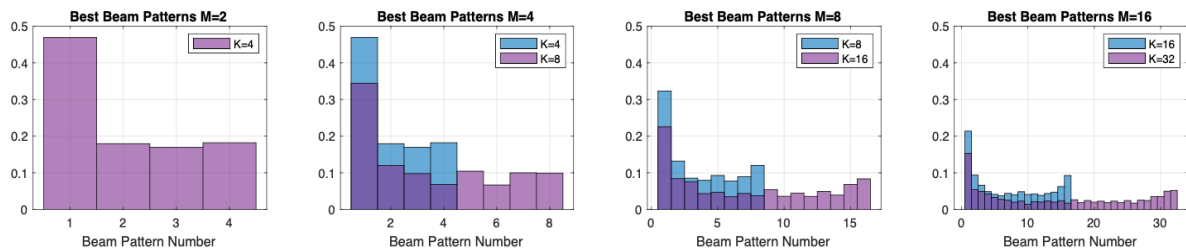


Figure 32 - Histogram. Frequency(percentage) each beam pattern is chosen as ‘best beam’ according to values of M and K. Blue represents K=M and purple denotes K=2M.

Figure 32 shows the percentage of times each beam pattern is selected as ‘best beam’. Best, in this context, denotes the highest gain as this relates to the Central BS antenna gain. The outcome of increasing the number of beam pattern options K is that the percentage of times a certain beam is chosen becomes slightly less dominant as there are more options to pick from, but with one particular beam pattern number still being preferred: beam pattern 1. This preference falls considerably as K increases: for K=4, beam pattern 1 is selected 16880 times, whereas for K=32 it is selected 5508 times.

## 5.2. Results

Since in Chapter 4 it was established that Case D is the closest to reality, it is the case used in this chapter along with the same mmWave Picocell parameters and SUI model. However, it is important to recognize that the randomness of Case D impairs the accuracy of results to some extent (e.g.: if  $K=M$  randomly picked a beam for an interfering BS that generates higher interference and  $K=2M$  happens to randomly pick one that generates lower interference, the results would be biased) - the variations are less than 3% on the mean cell throughput and less than 1% on the mean of other metrics.

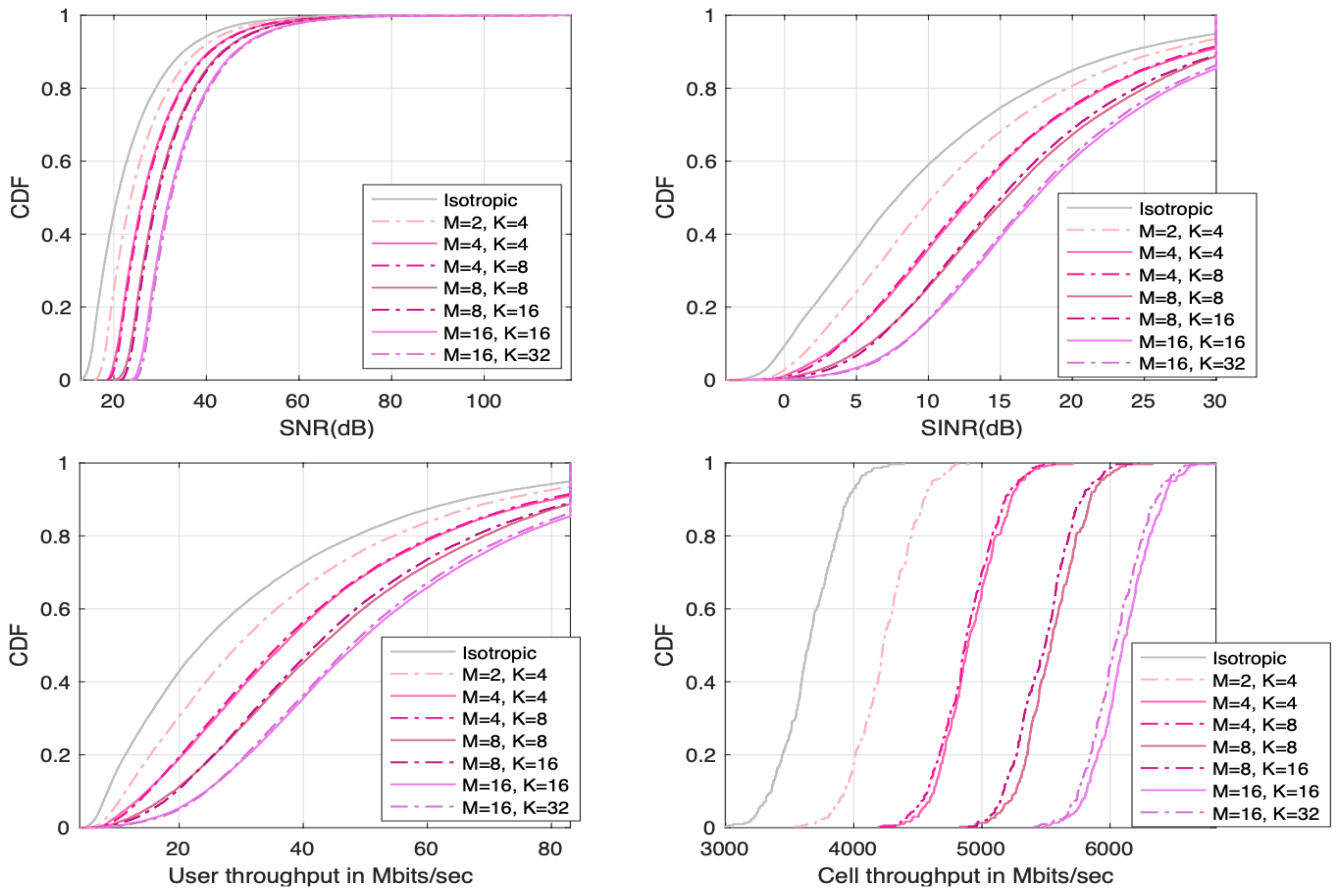


Figure 33 - mmWave Picocell, SUI model: CDF versus performance metrics. Various values of  $M$  and  $K$  are applied, and the selection of beams occurs according to **Case D**. Solid lines represent  $K=M$ , dashed lines represent  $K=2M$ .

According to what was discussed in Section 5.1,  $K=2M$  supposedly gives better results than  $K=M$ . This hypothesis is true for SNR, as seen in Figures 32 and 33. The randomness of Case D as it only affects the interference power, so the results of SNR do not suffer from that. The received power is boosted as  $M$  increases because the central BS selects beams that result in the highest gains, improving the SNR.

Modifying  $K=M$  to  $K=2M$  for  $M=4$  has a 0.87% in the average SNR, whereas this change for  $M=8$  improves it by 0.98% and for  $M=16$  it shows 1.07% improvement. This shows that narrower beams (due to larger M's) can benefit more from the better angular resolution offered by  $K=2M$ . This is even more evident for the maximum SNR values in Figure 34.

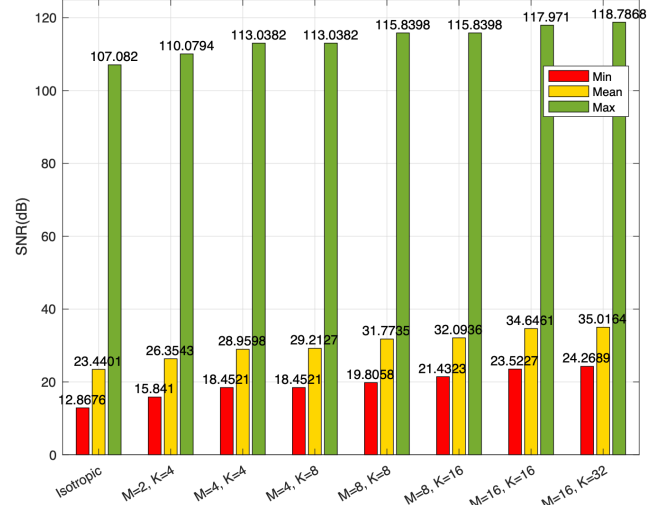


Figure 34 – mmWave Picocell, SUI model: Minimum, mean, and maximum SNR

A greater M increases the diversity and the maximum array gain, consequently increasing the wanted signal (received power). Therefore, the mean of every performance metric increases with M. Nonetheless, increasing M can also increase the interference (the minimum SINR using  $M=2$  is higher than that of  $M=4$ ) – the extent of this augmentation in interference is a matter of luck, as the selection of interfering beams occurs randomly.

After simulating the results several times, it is possible to confirm that the impact of randomness is not strong enough to alter the trend between  $K=M$  and  $K=2M$  seen in every simulation: the average SINR of  $K=M$  are greater than those of  $K=2M$ , but the minimum SINR of  $K=M$  are lower (how much lower depends on luck) – this is also true for cell throughput. This indicates that  $K=2M$  enhances the performance of users located at the cell-edge

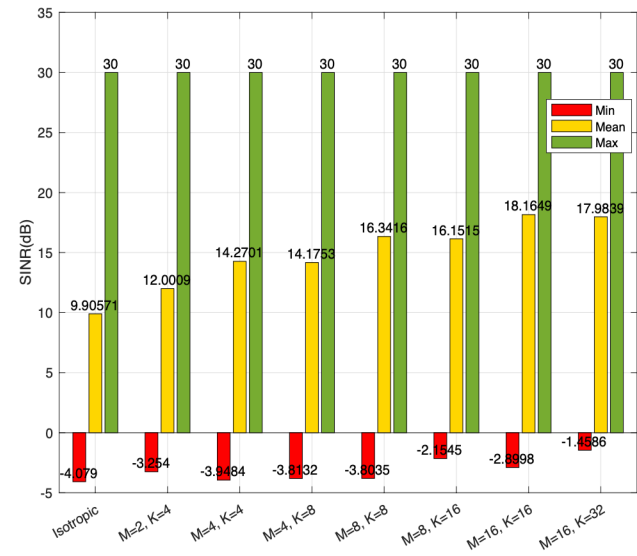


Figure 35 - mmWave Picocell, SUI model: Minimum, mean, and maximum SINR.

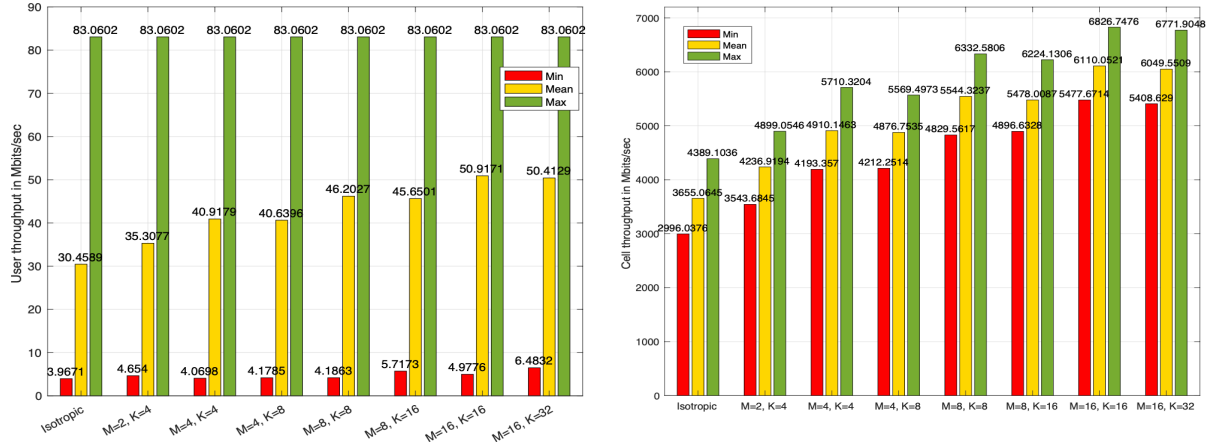


Figure 37 – mmWave Picocell, SUI model: Minimum, mean, and maximum user and cell throughputs.

As mentioned, Figure 36 shows that the user throughputs obtained with  $K=2M$  present a lower average than that of  $K=M$ , but a better the minimum value. This trend, conversely, is not seen on the cell throughput as this metric is not on a per-user basis. The performance metrics can be observed in more detail in Figure 37, where this data is displayed in the form of histograms.

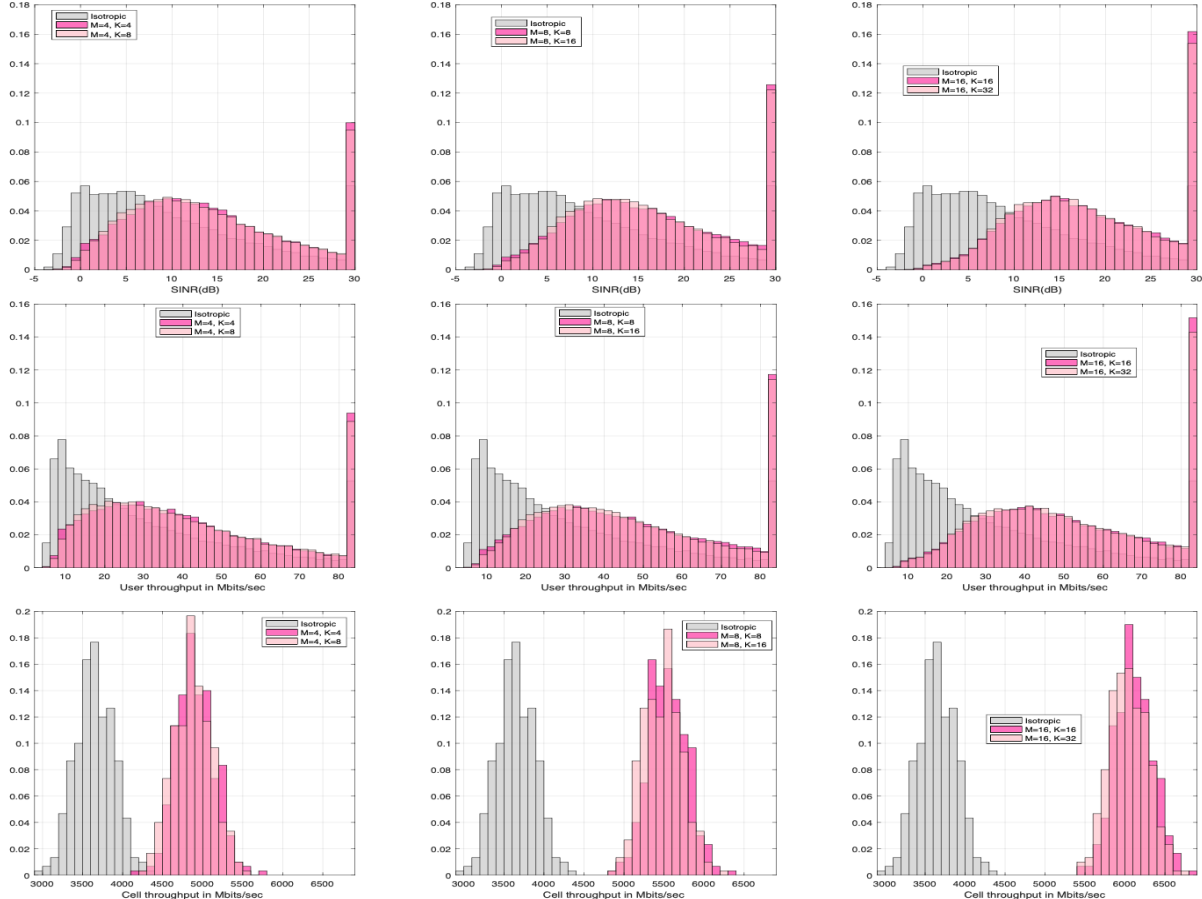


Figure 36 – mmWave Picocell, SUI model: Histograms. Frequency (percentage) of occurrence versus

### **5.3. Conclusion**

$K=2M$  does not result in improvements for the cell, but it does make a difference in terms of outage as it boosts the performance of the worst users (users at cell-edge) which is important for user fairness in a network. When using  $K=2M$ , the minimum user throughput increases 2.67% for  $M=4$  - this value is for  $M=8$  and  $M=16$  is 36.6% and 30.2%, respectively. This comes at the cost of decreasing the average user and cell throughputs by 0.68%, 1.2%, and 0.99% for  $M=4$ ,  $M=8$ , and  $M=16$ .

Using double the number of antenna elements can result in an extra 570-680 Mbits/sec to the cell throughput average, but this comes at a cost. When deciding whether or not to increase the number of antenna elements, this choice should be made considering not only the benefits resulting from better diversity and higher maximum array gains but also pondering the trade-off in terms of aspects of the transmitter such as complexity, device size, and price.

## Chapter 6.

# Double-Directional Beamforming

According to [5], increasing the number of antenna results in better coverage. Applying beamforming at the receiver to obtain double-directional beamforming implies multiple antennas on the Rx side as well as on the Tx side, thus increasing the number of antennas. Therefore, the number of receiver antennas is at least double the number of antennas used for an isotropic receiver.

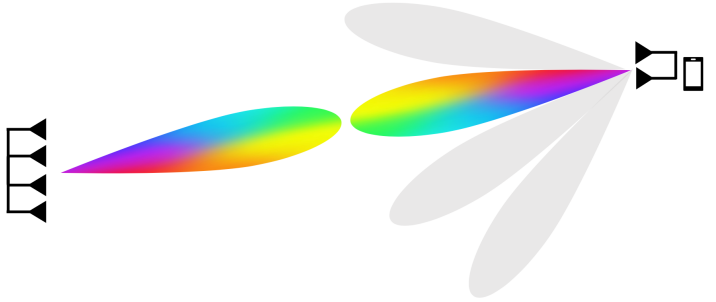


*Figure 38 - Downlink MIMO using antenna array of 2 antenna elements to generate 4 beam patterns on the Rx side, and antenna array of 4 antenna elements to generate 8 beam patterns (one has already been selected) on the Tx side. Image created by the author, inspired by [70]*

For this thesis, the chosen antenna for the receiver side is an antenna array of 2 antenna elements ( $M=2$ ) to generate 4 beam patterns ( $K=4$ ). The configurations of the transmitter side remain the same as they were in Chapter 4: an antenna array of 4 antenna elements ( $M=4$ ) to generate 4 beam patterns ( $K=8$ ). Additionally, transmit beamforming (one directional, without receive beamforming) using  $M=8$  and  $K=16$  on the transmitter is also considered. The intent is to compare the benefits of doubling the number of antennas on the receiver side to obtain double-directional beamforming ( $Tx+Rx$ ) with the benefits of doubling the number of antennas on the transmitter side for transmit beamforming only.

Double-directional beamforming provides increased diversity for the BS and UE. For this study, the system is considered a Single-User Multiple-Input-Multiple-Output (SU-MIMO) as there are multiple antennas on both ends and beams are selected individually for each user (Single-User). The beam selection does not consider the position of other users (it only considers the position of the interfering BSs) and whether or not a beam's side lobe pointing at another user is causing more intra-cell interference.

The central and interfering transmitter beams are selected first, exactly as they were in Case D from Chapter 4. Then, the receiver beams are selected given the current transmit beam using a mechanism focusing on one specific performance metric: SNR or SINR. The SINR exhaustive search developed is performed only on the receive side, as implementing it simultaneously on both sides would be a much more complex task that would also increase the search time making it too time-consuming.

Similarly to [39], the SINR exhaustive search (max-SINR) takes the trade-off between maximizing gain and minimizing interference into consideration, while the SNR mechanism (max-SNR) has the exclusive goal of maximizing gain so it simply selects the beams that result in the highest array factors – it does not require exhaustive search.

## 6.1. Results

Figure 39 confirms that both methods achieve their goals of boosting the specified metrics: max-SNR technique has the best SNR, max-SINR search has the best SINR and, consequently, user and cell throughputs. According to the overall results, applying ‘Tx+Rx’ beamforming, which doubles the number of Rx antennas (by applying Rx beamforming to the existing Tx beamforming), is more advantageous than doubling the number of Tx antennas for ‘Tx only’ beamforming.

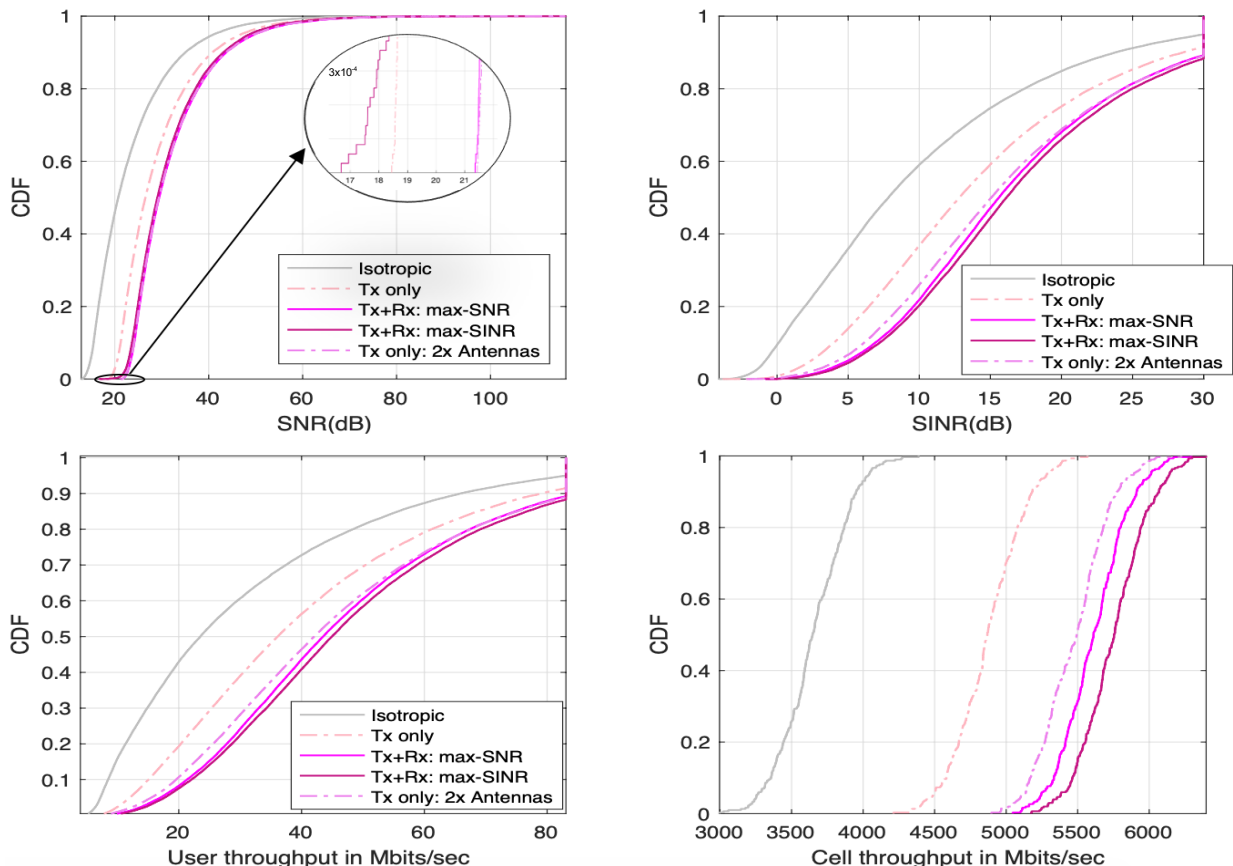


Figure 39 - mmWave Picocell, SUI model: CDF versus performance metrics.

This does not imply that Rx beamforming is superior to Tx beamforming as an ‘Rx only’ beamforming option was not discussed in this thesis. What is shown is that the combination of Tx and Rx beamforming is more appealing than just Tx beamforming (with twice as many Tx antennas or not), revealing the importance of diversity on both ends.

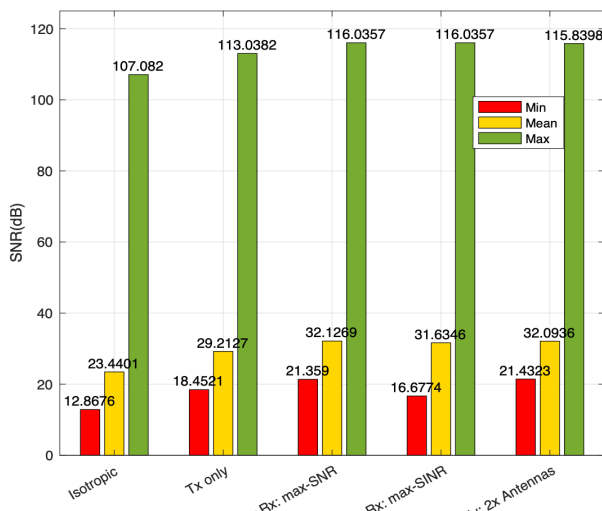


Figure 40 – mmWave Picocell, SUI model: Minimum, mean, and maximum SNR

The max-SINR approach has a worse SNR for cell-edge users than that achieved with ‘Tx only’ – this is due to the previously mentioned trade-off of the SINR exhaustive search. Figure 39 shows that the max-SNR approach gives the best overall results for the metric that it intends to improve (SNR), but it is overtaken by very little in terms of cell-edge users by Tx only: 2x Antennas.

As predicted, the SINR exhaustive search method gives the best result for SINR in Figure 40. Unlike what was seen for SNR, both double-directional beamforming search methods give much better SINR results than using twice the number of Tx antennas for transmit beamforming. Using only Tx beamforming increases the cell-edge users SINR by 6.5% relative to isotropic. Doubling the number of Tx antennas for Tx only brings this value to 47.2%.

As discussed in Chapter 4, Tx beamforming with  $M=4 K=8$  improved the mean SNR value by 24.6% compared to isotropic. Tx only: 2x Antennas, with  $M=8 K=16$ , adds 12.3% (36.9%). Double-directional beamforming with Tx+Rx:  $M=4 K=8 + M=2 K=4$  brings this value to 37.1%, representing an extra 12.5% when using the max-SNR method, whereas the max-SINR search increases it by only 10.36% (34.96%). These percentages of improvement were calculated from the values shown in Figure 39.

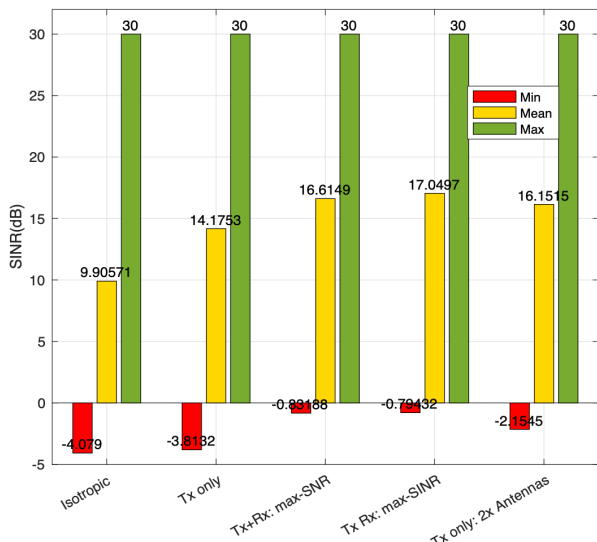


Figure 41 – mmWave Picocell, SUI model: Minimum, mean, and maximum SINR

The double-directional beamforming max-SNR and max-SINR methods, however, boost the improvement in SINR for cell edge users to 79.6% and 80.5%, respectively. The significant discrepancy between the improvements resulting from doubling the Tx antennas for Tx only and using either of the Tx+Rx beamforming search methods suggest that the latter is a much superior solution to enhancing the SINR of users located at the cell-edge.

A similar trend is seen for the user throughput of cell-edge users. As analysed in Chapter 4, both cell and user throughputs have an overall increase of 33.4% with ‘Tx only’ beamforming. This value reaches 49.9% when using twice as many Tx antennas. For the Tx+Rx beamforming max-SNR and max-SINR approaches, the enhancements of mean throughputs reach 56.9% and 57.4%, respectively. These calculations were performed with the values from Figure 41.

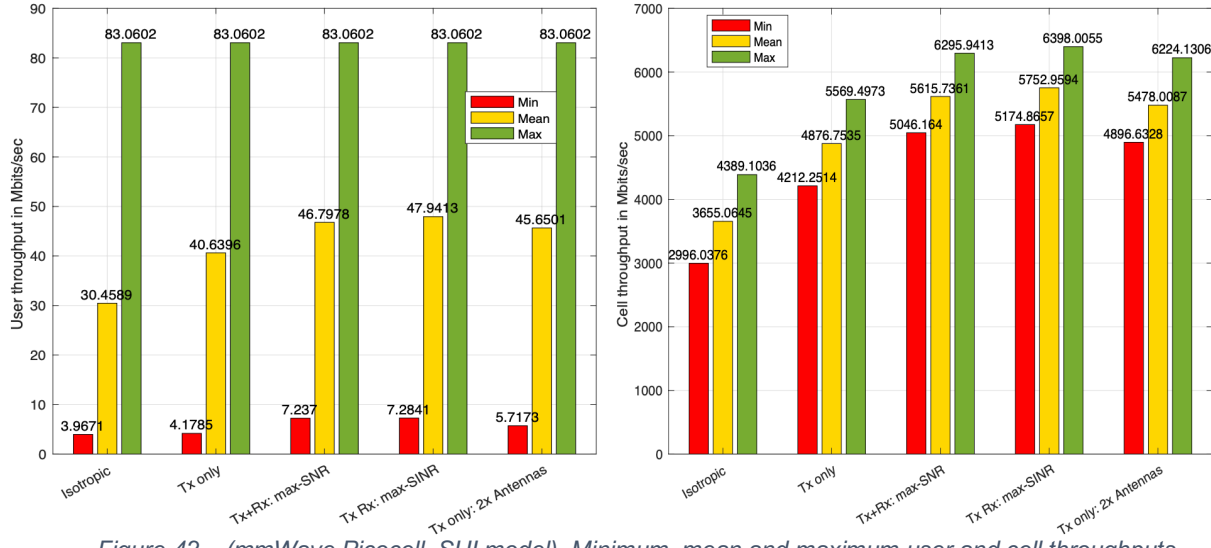


Figure 42 – (mmWave Picocell, SUI model). Minimum, mean and maximum user and cell throughputs

## 6.2. Conclusion

The minor difference between the double-directional beamforming methods overall results suggests that both max-SNR and max-SINR are extremely advantageous for users located at the cell-edge. Transmit beamforming with twice as many antennas has proven to be approximately as good as max-SNR in terms of SNR results, but it falls behind when it comes to other metrics.

When choosing double-directional beamforming, the decision regarding which selection method (max-SNR or max-SINR) to use could rely mostly on what performance metric needs to be improved the most, as the max-SNR’s and max-SINR’s overall improvements differ very little from each other. However, max-SINR method poses a potential drawback: as it entails an exhaustive

search, it certainly takes longer than the max-SNR approach. The time taken to perform the max-SNR is 80.2 seconds, whereas max-SINR takes 292.1 seconds. Therefore, if the intent is to maximise SNR whilst significantly improving the other performance metrics too, max-SNR could be a good compromise in terms of results and time. But there are other aspects to consider in terms of feasibility.

From a practical perspective, changing from isotropic to double-directional beamforming can be seen as doubling the number of antenna elements on the receive side (isotropic uses  $M=1$  and the Tx+Rx beamforming for this thesis uses  $M=2$ ) by adding only 1 antenna, whereas Tx: 2x Antennas is doubling the number of antenna elements of transmit beamforming but this is achieved by adding 4 antennas rather than 1. Usually, adding 1 antenna at the receiver would be easier than adding 4 antennas to the transmitter. Nonetheless, the number of receivers must be considered for each particular circumstance: this thesis, for example, has 120 users for each cell and thus, 120 receivers for every basestation. Manufacturing 120 extra antennas so that each receiver has  $M=2$  antenna elements might be considerably more expensive than producing 4 antennas for each basestation (7 basestations in total for this thesis).

Hence, the circumstances should be considered and the final decision on whether the number of antenna elements should be doubled at the transmitter for transmit beamforming or at the receiver for double-directional beamforming should be pondered as mentioned on Chapter 5, considering trade-offs in terms of improvement, device size, price, time, and any other criteria that might be relevant.

## **Chapter 7.**

### **Conclusions**

Throughout this thesis, the advantages of beamforming using IEEE 802.15.3c codebooks for a homogenous cellular network were assessed. Initially, three simulation scenarios (Macro, Micro and mmWave Picocell) were considered but the focus was on the mmWave Picocell. The performance metrics calculated were SNR, SINR, user throughput and cell throughput.

In Chapter 3, several propagation path loss models were analysed. For an accurate link budget calculation, the most suitable model has to be selected and considering the main simulation scenario of this thesis, mmWave Picocell, the model selected for this study was Stanford University Interim (SUI).

Chapter 4 examined four distinct transmit beamforming cases by investigating their merits and levels of accuracy. Transmit beamforming has proven to fulfil its purpose of minimising the interference while maximising the received power. The key takeaway from this chapter is that uncoordinated beamforming at the transmitter enhances the user (including those located at the cell-edge) performance as well as the cell performance and coordinated beamforming has the potential of improving it even more. However, it is important to consider that the latter would require intercell communication and this would potentially increase the complexity of communication between cells and the protocols they use to cooperate.

In Chapter 5, the advantages and disadvantages of changing the values of antenna elements and beam patterns were inspected, including their relations of  $K=M$  or  $K=2M$ . While it is true that mmWave frequencies enable the use of large antenna arrays and that doubling antenna elements can offer an extra 570-680 Mbits/sec to the mean cell throughput, it comes at a cost. Having twice as many antenna elements means that the antenna array will occupy more space and it makes the device more complex and expensive. According to the results, it is recommended to use  $M=2$ ,  $8$  or  $16$  considering the performance of users located at cell edge. The decision of whether to use  $K=M$  or  $K=2M$  should be taken considering the trade-off between average user performance and minimum user performance:  $K=M$  has a better performance in terms of the cell, in exchange for a worse performance for edge users.  $K=2M$  has a better performance for these users, at the expense of worse

average for the cell and possibly longer switch time. If the main goal is to improve fairness by enhancing the performance of users at the cell-edge,  $K=2M$  should be chosen.

Chapter 6 suggests a max-SINR and max-SNR approaches for the Rx beam selection - given that the Tx beam has already been selected - in double-directional (Tx+Rx) beamforming. Each of these approaches was compared to the transmit beamforming (Tx only) using  $K=2M$  and to transmit beamforming with an  $M$  twice as large (Tx only: 2x Antennas). It was proved that the double-directional options perform significantly better than the transmit beamforming on its own. Yet, the main discovery in this chapter is that when doubling the number of antenna elements in Tx beamforming, the results overall are not that much inferior those of 'Tx+Rx'. Double-directional beamforming entails using twice as many antennas (compared to the number of Rx antennas used on 'Tx only') on the Rx side. Even though 'Tx+Rx' presents superior results compared to those obtained with 'Tx only' approaches, the decision of whether to implement one or the other should not be based solely on these results. This decision should be made considering many aspects such as metric that needs to be enhanced, complexity, price, size, search time, number of users and number of basestations.

## 7.1. Future Work

Further work could focus on some of the project limitations: the software developed only simulates homogeneous cellular networks, only populates the cell of interest, does not consider some of the mmWave's additional losses (e.g.: attenuation due to rain) and does not take antenna heights into consideration when calculating the angles of arrival and departure. Inter-cell communication could also be implemented. These are some of the aspects that could be further improved in order to obtain more accurate results.

Some of the software's capabilities could be used to further investigate the difference in results in terms of environments such as urban, suburban and rural. The impact of changes in Tx and Rx antenna heights could also be conducted in order to evaluate the accuracy of the models currently available. Moreover, real measurements could be obtained, and these could be compared to the results simulated as a way of assessing which model is actually closer to reality.

There are many aspects of beamforming that could be further explored:

- Study of receive beamforming on its own could be conducted in order to determine whether transmit beamforming is more advantageous than receive beamforming or vice-versa.
- Develop an improved codebook protocol, with minimum loss at the intersection of two beams, or apply other existing codebooks (e.g.: circular codebook) to analyse the contrast in results.
- Analyse how the chosen uniform spacing between antennas can impact the results by choosing values other than  $\lambda/2$ .
- Exhaustive search could be jointly implemented on the Tx and Rx side to find the ‘ultimate optimal beams’ and compare the results with the existing max-SINR and max-SNR techniques to confirm whether better accuracy in results is worth the extra time and complexity that the full exhaustive search needs.
- Only a certain range of possible M values was examined. One could evaluate the additional gain of applying much larger values of M at both ends of the link.
- Close examination of the results obtained for the other simulation scenarios, analysing whether the improvement for beamforming changes at different scenarios (e.g.: different cell sizes or carrier another frequency as in [65]).
  - The benefits of realistic coordinated/cooperative using different resources could be investigated after implementing inter-cell communication into the software.

## Mitigation plan

Event/Issue	Potential/actual Impact on project	Action(s) taken to mitigate impact on outcomes	Remaining impact
	<ul style="list-style-type: none"><li>- Connectivity issues during meetings with the supervisor.</li><li>- Time zone difference of 4 hours between Brazil and the United Kingdom.</li><li>- Change of circumstances (e.g.: spending 1.5 weeks in a farm, where there was no signal) disrupted the student's working pattern.</li></ul>	<p>Move the meetings to emails when needed. Find a suitable time for both the student and her supervisor.</p>	N/A

## References

- [1] R. K. J. Akhil Gupta, "A Survey of 5G Network: Architecture and Emerging Technologies," *IEEE Access*, vol. 3, pp. 1206-1232, 2015.
- [2] P. A. Nix, Mobile Communications, University of Bristol, 1994-2018.
- [3] M. H. Alsharif, A. H. Kelechi, M. A. Albreem, S. A. Chaudhry, M. S. Zia and a. S. Kim, "Sixth Generation (6G) Wireless Networks: Vision, Research Activities, Challenges and Potential Solutions".
- [4] E. Ali, M. Ismail, R. Nordin and N. F. Abdulah, "Beamforming techniques for massive MIMO systems in 5G: overview, classification, and trends for future research," *Frontiers of Information Technology & Electronic Engineering*, vol. 18, p. 753–772, 2017.
- [5] H. Holma, A. Toskala and T. Nakamura, 5G Technology: 3GPP New Radio, 2019.
- [6] J. S. Kim, W. J. Lee and M. Y. Chung, "A Multiple Beam Management Scheme on 5G Mobile Communication Systems for Supporting High Mobility".
- [7] U. Karabulut, A. Awada, A. Lobinger, I. Viering, M. Simsek and G. P. Fettweis, "Average Downlink SINR Model for 5G mmWave Networks with Analog Beamforming," in *IEEE Wireless Communications and Networking Conference (WCNC)*, Barcelona, 2018.
- [8] A. Borna, "Interference Management Techniques for Multi-Standard Wireless Receivers," University of California, Berkeley, 2012.
- [9] A. B. Carlson and P. B. Crilly, Communication Systems An Introduction to Signals and Noise in Electrical Communication, 2010.
- [10] International Telecommunication Union, "BT.1368: Planning criteria for digital terrestrial television services in the VHF/UHF bands".
- [11] R. C. V. Macario, Cellular Radio Principles and Design, MACMILLAN PRESS LTD, 1997.
- [12] M. Rebato, M. Mezzavilla, S. Ranga, F. Boccardi and M. Zorzi, "Understanding Noise and Interference Regimes in 5G Millimeter-Wave Cellular Networks," *ArXiv*, vol. 1604.05622, 2016.
- [13] A. Goldsmith, "Cellular Systems and Infrastructure-Based Wireless Networks," in *Wireless Communications*, 2005, pp. 505-534.
- [14] I. Mohamed, "Path-Loss Estimation for Wireless Cellular Networks Using Okumura/Hata Model," *Science Journal of Circuits, Systems and Signal Processing*, vol. 7, no. 1, pp. 20-27, 2018.
- [15] S. Armour, "Communications 2EN/3S (EENG 22000 / EENG 22010)," University of Bristol.

- [16] A. Arun and T. K. Sreeja, "An Effective Downlink Budget for 2.24GHz S-Band LEO Satellites," in *IEEE Conference on Information & Communication Technologies*, 2014.
- [17] M. R. Akdeniz, Y. Liu and M. K. Samimi, "Millimeter Wave Channel Modeling and Cellular Capacity Evaluation," *IEEE Journal on Selected Areas in Communications*, vol. 32, no. 6, pp. 1164-1179, 2014.
- [18] R. Hasan, M. M. Mowla, M. A. Rashid, M. K. Hosain and I. Ahmad, "A Statistical Analysis of Channel Modeling for 5G mmWave Communications," in *International Conference on Electrical, Computer and Communication Engineering (ECCE)*, Bangladesh, 2019.
- [19] A. Goldsmith, *Wireless Communications*, Stanford University, 2004.
- [20] H. Sun and R. Q. Hu, *Heterogeneous Cellular Networks*.
- [21] L. Liu, J. Zhang, J.-C. Yu and J. Lee, "Intercell Interference Coordination through Limited Feedback," *International Journal of Digital Multimedia Broadcasting*, 2010.
- [22] D. G. Uwakwe, A. A. Ajani, O. Rowani and a. A. N. Isaac-Ugbogu, "The evaluation of the impact of Inter-Cell Interference Coordination on the performance of users in an LTE system," in *Proceedings of the Sustainable Research and Innovation Conference*, Kenya, 2018.
- [23] M. C. Valenti, "The Wireless Networking Workbook," West Virginia University, 2018.
- [24] A. F. Molisch, *Wireless Communications*, Wiley-IEEE Press, 2010.
- [25] M. S. Mollel and M. Kisangiri, "Comparison of Empirical Propagation Path Loss Models for Mobile Communication," *Computer Engineering and Intelligent Systems*, vol. 5, no. 9, 2014.
- [26] M. Ekpenyong, J. Isabona and E. Ekong, "On Propagation Path Loss Models For 3-G Based Wireless Networks: A Comparative Analysis," *Georgian Electronic Scientific Journal: Computer Science and Telecommunications* , vol. 2, pp. 74-84, 2010.
- [27] G. L. Stuber, *Principles of mobile communication*, Kluwer Academic Publishers, 2002.
- [28] A. Bhuvaneshwaria, R. Hemalathab and T. Satyasavithric, "Semi Deterministic Hybrid Model for Path Loss Prediction Improvement," *Procedia Computer Science*, vol. 92, pp. 336-344, 2016.
- [29] G. Çelik, H. Çelebi and G. Tuna, "A novel RSRP-based E-CID positioning for LTE networks," in *International Wireless Communications and Mobile Computing Conference (IWCMC)*, Valencia, 2017.
- [30] J. Lempäinen and M. Manninen, "Radio Propagation Prediction," in *Radio Interface System Planning for GSM/GPRS/UMTS*, 2002.
- [31] R. Rahul, B. Bansal and R. Kapoor, "Performance Analysis of Empirical Radio Propagation Models in Wireless Cellular Networks," *World Scientific News*, vol. 121, pp. 40-46, 2019.

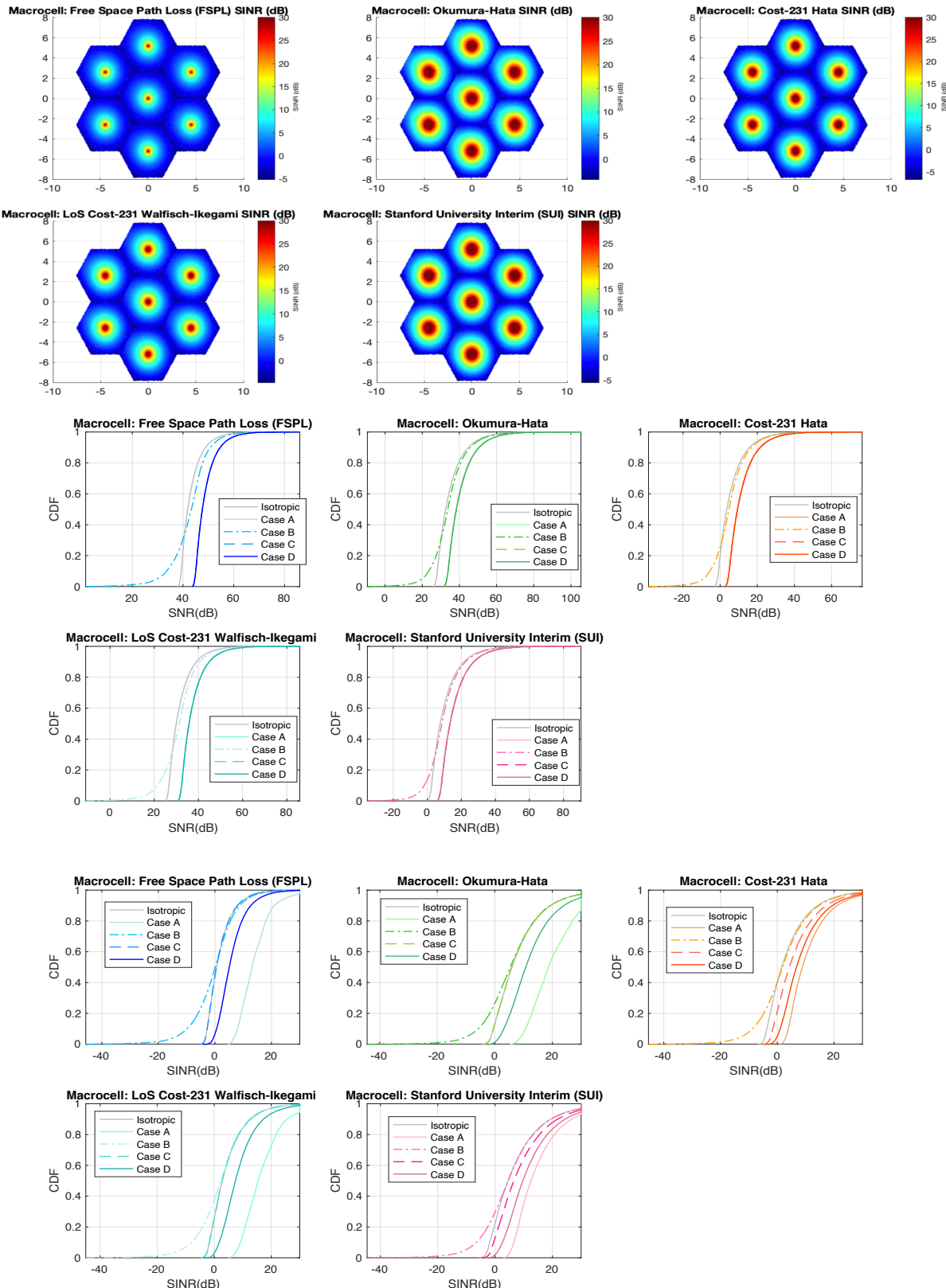
- [32] V. Abhayawardhana, I. Wassell, D. Crosby, M. Sellars and M. Brown, "Comparison of Empirical Propagation Path Loss Models for Fixed Wireless Access Systems," in *IEEE 61st Vehicular Technology Conference*, Stockholm, 2005.
- [33] W. Lambrechts and S. Sinha, Last Mile Internet Access for Emerging Economies.
- [34] A. I. Sulyman, A. T. Nassar, M. K. Samimi, G. R. M. Jr., T. S. Rappaport and A. Alsanie, "Radio Propagation Path Loss Models for 5G Cellular Networks in the 28 GHz and 38 GHz Millimeter-Wave Bands," *IEEE Communications Magazine*, pp. 78-86, 2014.
- [35] B. Kamali, eroMACS: An IEEE 802.16 Standard-Based Technology for the Next Generation of Air Transportation Systems, John Wiley & Sons, 2018.
- [36] A. Dimas, D. Kalogerias and A. P. Petropulu, "Cooperative Beamforming With Predictive Relay Selection for Urban mmWave Communications," *IEEE Access*, vol. 7, 2019.
- [37] A. M. A. Abdo, X. Zhaoa and A. Ahmeda, "Codebooks design and performance evaluation based on antenna array response and signal to noise ratio for mmWave communication," *Journal of International Council on Electrical Engineering*, vol. 8, no. 1, p. 163–171, 2018.
- [38] K. Fugimoto, Mobile Antenna Systems Handbook, Artech House Publishers, 2nd.
- [39] X. Yu, S. M. D. Armour and C. Yu, "Codebook Based Self-Adaptive Beamforming for 5G Rail Communications," in *IEEE International Conference on Signal Processing (ICSP)*, Beijing, 2018.
- [40] A. Al-Dulaimi, X. Wang and C.-L. I, 5G Networks: Fundamental Requirements, Enabling Technologies, and Operations Management, John Wiley & Sons, 2018.
- [41] Z. Liu, W. u. Rehman, X. Xu and X. Tao, "Minimize Beam Squint Solutions for 60GHz Millimeter-wave Communication System," in *Vehicular Technology Conference*, Las Vegas, NV, USA, 2013.
- [42] *Wireless Medium Access Control (MAC) and Physical Layer (PHY) Specifications for High Rate Wireless Personal Area Networks (WPANs), Amendment 2: Millimeter-Wave-Based Alternative Physical Layer Extension, IEEE Standard 802.15.3c*, 2009.
- [43] W. Yuan, S. M. D. Armour and A. Doufexi, "An Efficient and Low-complexity Beam Training Technique for mmWave Communication," in *Annual International Symposium on Personal, Indoor, and Mobile Radio Communications (PIMRC)*, Hong Kong, China, 2015.
- [44] W. Feng, Z. Xiao, D. Jin and L. Zeng, "Circular-Antenna-Array-Based Codebook Design and Training Method for 60GHz Beamforming," *IEEE Wireless Communications and Networking Conference (WCNC): PHY*, pp. 4140-4145, 2013.
- [45] J. Wang and e. Al., "Beamforming Codebook Design and Performance Evaluation for 60GHz Wideband WPANs," *IEEE Vehicular Technology Conference Fall*, vol. 70, pp. 1-6, 2009.
- [46] J. Mo and e. Al, "Beam Codebook Design for 5G mmWave Terminals," *IEEE Access*, vol. 7, pp. 1-17, 2019.

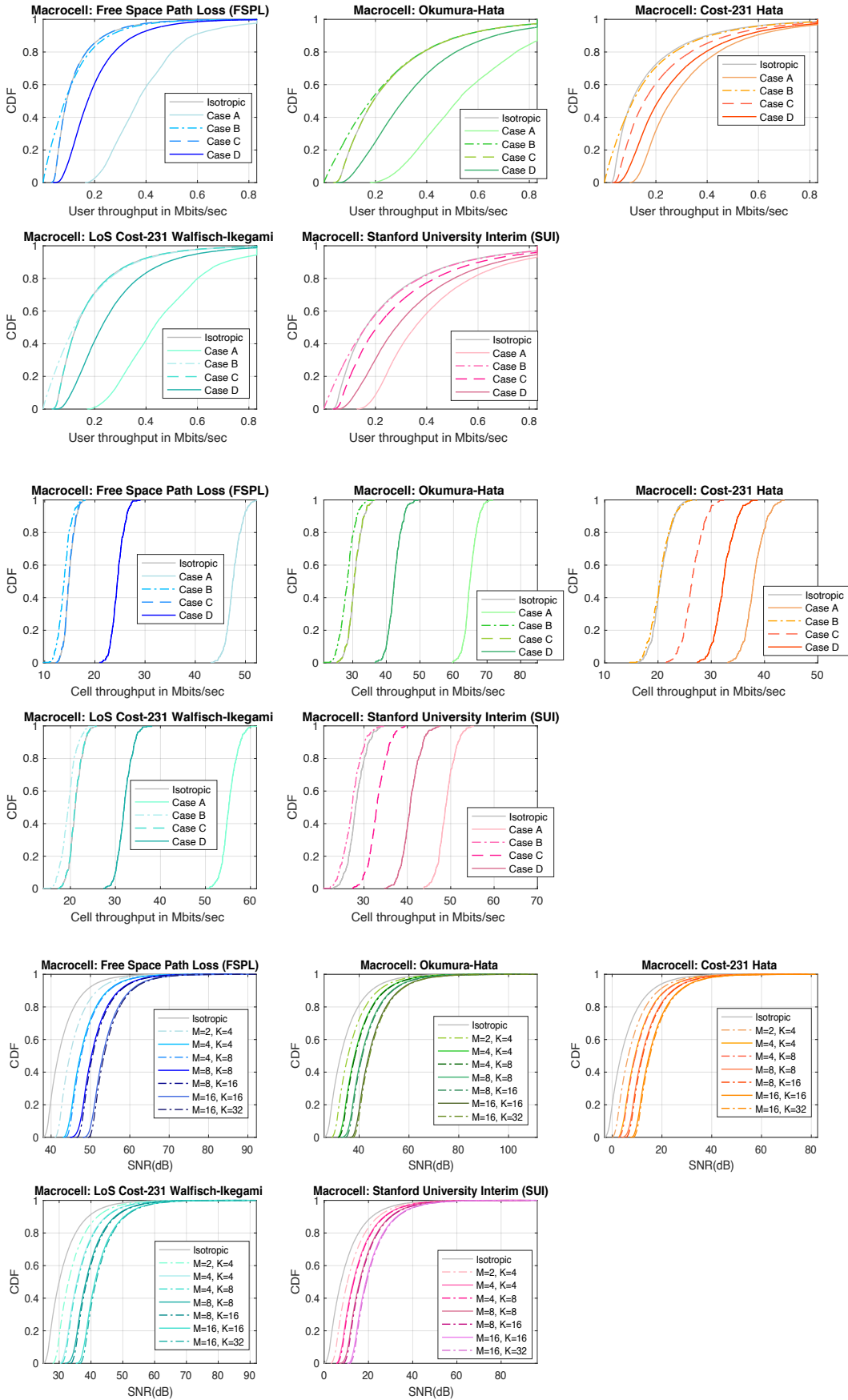
- [47] X. Liu and A. O. Fapojuwo, "Performance analysis of hierarchical cellular networks with queueing and user retrials," *International Journal of Communications Systems*, vol. 19, pp. 699-721, 2006.
- [48] L. C. Godara, *Handbook of Antennas in Wireless Communications*.
- [49] R. Esmailzadeh, *Broadband Wireless Communications Business: An Introduction to the Costs and Benefits of New Technologies*.
- [50] "Chapter - 2 Small Cell Cellular Network," [Online]. Available: [https://shodhganga.inflibnet.ac.in/bitstream/10603/141885/7/07\\_chapter2.pdf](https://shodhganga.inflibnet.ac.in/bitstream/10603/141885/7/07_chapter2.pdf). [Accessed 30 April 2020].
- [51] Q. Mu, L. Liu, L. Chen and Y. Jiang, "CQI table design to support 256 QAM in small cell environment," *International Conference on Wireless Communications and Signal Processing*, 2013.
- [52] W. Gao, *Energy and Bandwidth-Efficient Wireless Transmission*.
- [53] V. Garg, *Wireless Communications & Networking*, Morgan Kaufmann, 2007.
- [54] D. T. Ngo, D. H. N. Nguyen and T. Le-Ngoc, "Chapter 6 - Intercell Interference Coordination: Towards a Greener Cellular Network," in *Handbook of Green Information and Communication Systems*, 2013, pp. 147-182.
- [55] G. R. MacCartney and T. S. Rappaport, "Study on 3GPP Rural Macrocell Path Loss Models for Millimeter Wave Wireless Communications," in *IEEE International Conference on Communications (ICC)*, Paris, 2017.
- [56] S. Catteux, P. F. Driessen and L. J. Greenstein, "Data throughputs using Multiple-Input Multiple-Output (MIMO) techniques in a noise-limited cellular environment," *IEEE TRANSACTIONS ON WIRELESS COMMUNICATIONS*, vol. 1, no. 2, pp. 226-235, 2002.
- [57] N. Rakesh and D. Nalineswari, "Comprehensive performance analysis of path loss models on GSM 940 MHz and IEEE 802.16 WiMAX frequency 3.5 GHz on different terrains," in *International Conference on Computer Communication and Informatics (ICCCI)*, Coimbatore, 2015.
- [58] G. S. Bola and G. S. Saini, "Path Loss Measurement and Estimation Using Different Empirical Models For WiMax In Urban Area," *International Journal of Scientific & Engineering Research*, vol. 4, no. 5, pp. 1421-1428, 2013.
- [59] S. Sharma and S. Parashar, "Analysis of Path Loss Models at 3.3GHz to Determine Efficient Handover in Wimax," *International Journal of Engineering Research & Technology (IJERT)*, vol. 3, no. 7, pp. 45-51, 2014.
- [60] U. Türke, *Efficient Methods for WCDMA Radio Network Planning and Optimization*.

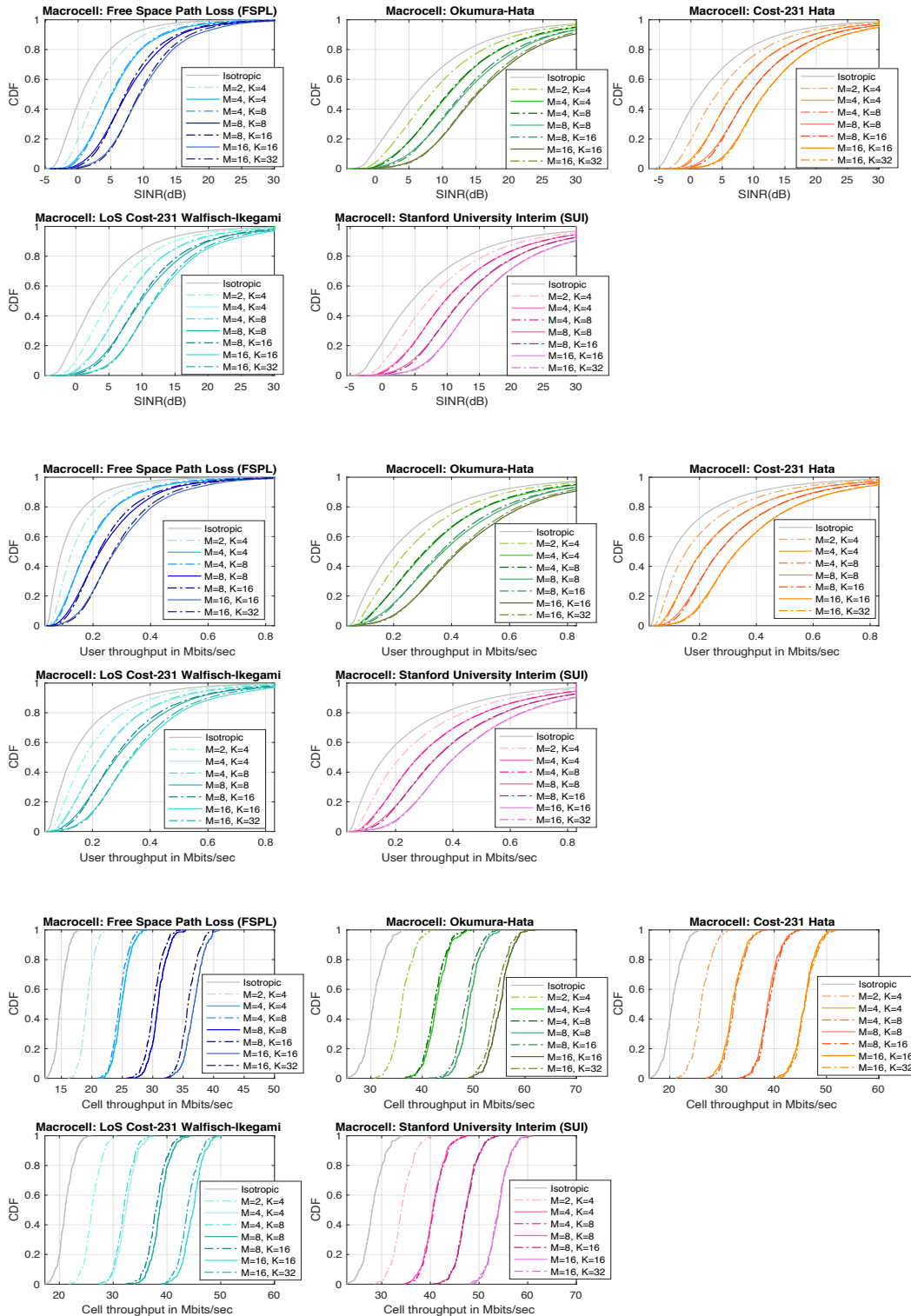
- [61] E. Aryafar, M. Khojastepour, K. Sundaresan, S. Rangarajan and E. W. Knightly, "ADAM: an adaptive beamforming system for multicasting in wireless LAN," *IEEE/ACM Transactions on Networking*, vol. 21, no. 5, 2013.
- [62] M. Vondra, E. Dinc and C. Cavdar, "Coordinated Resource Allocation Scheme for 5G Direct Air-to-Ground Communication," in *European Wireless*, Catania, 2018.
- [63] R. Zakhour, Z. K. M. Ho and D. Gesbert, "Distributed Beamforming Coordination in Multicell MIMO Channels".
- [64] S. G. Glisic, Advanced Wireless Networks: Technology and Business Models.
- [65] S. Z. et al., "Impact of BS Antenna Number and Array Geometry on Single-User LTE-A Data Throughputs in Realistic Macro and Pico Cellular Environments," in *IEEE Wireless Communications and Networking Conference (WCNC)*, New Orleans, 2015.
- [66] A. J. Sachin S. Kale, "Performance Analysis of Empirical Propagation models for WiMAX in Urban Environment," *IOSR Journal of Electronics and Communication Engineering (IOSR-JECE)*, vol. 1, pp. 24-28, 2012.
- [67] Y. Xiao, K. Sun, W. Huang, S. Meng, M. Wang and B. Wang, "Angle Sweeping and Scheduling in Downlink Opportunistic Beamforming Systems," in *International Conference on Communications and Networking in China (CHINACOM)*, Guilin, 2013.
- [68] N. Lemieux and M. Zhao, "Small Cells, Big Impact: Designing Power Solutions for 5G Applications," Texas Instruments.
- [69] J. D. Matyas, F. Hu and S. Kumar, *Wireless Network Performance Enhancement Via Directional Antennas: Models, Protocols, and Systems*, CRC Press, 2015.
- [70] E. Dahlman, S. Parkvall and J. Skold, *5G NR: The Next Generation Wireless Access Technology*, Mara Conner, 2018.
- [71] M. Cai, J. N. Laneman and B. Hochwald, "Beamforming Codebook Compensation for Beam Squint with Channel Capacity Constraint," in *IEEE International Symposium on Information Theory (ISIT)*, Aachen, 2017.

## Appendix A.

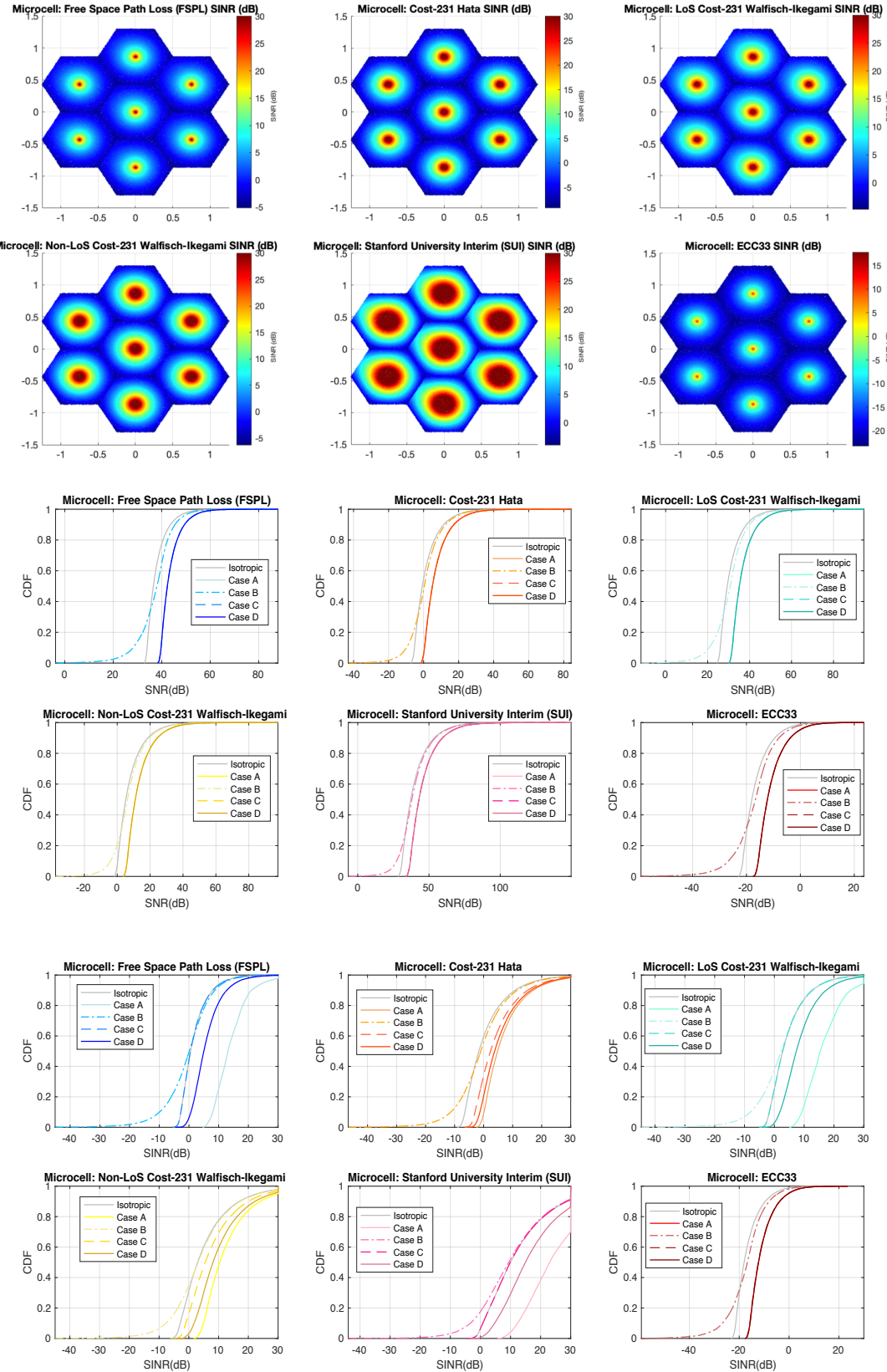
### Macrocell simulation

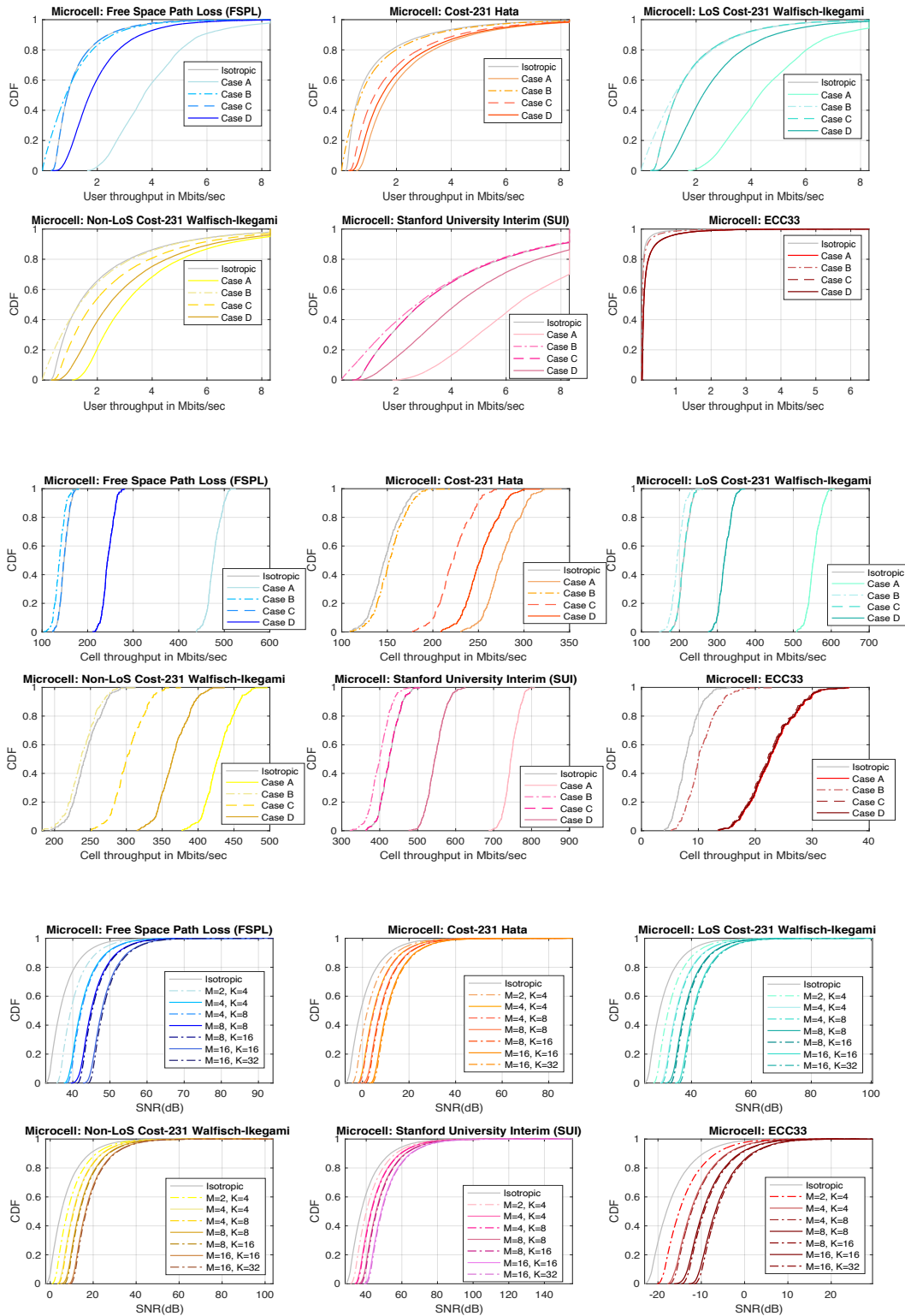


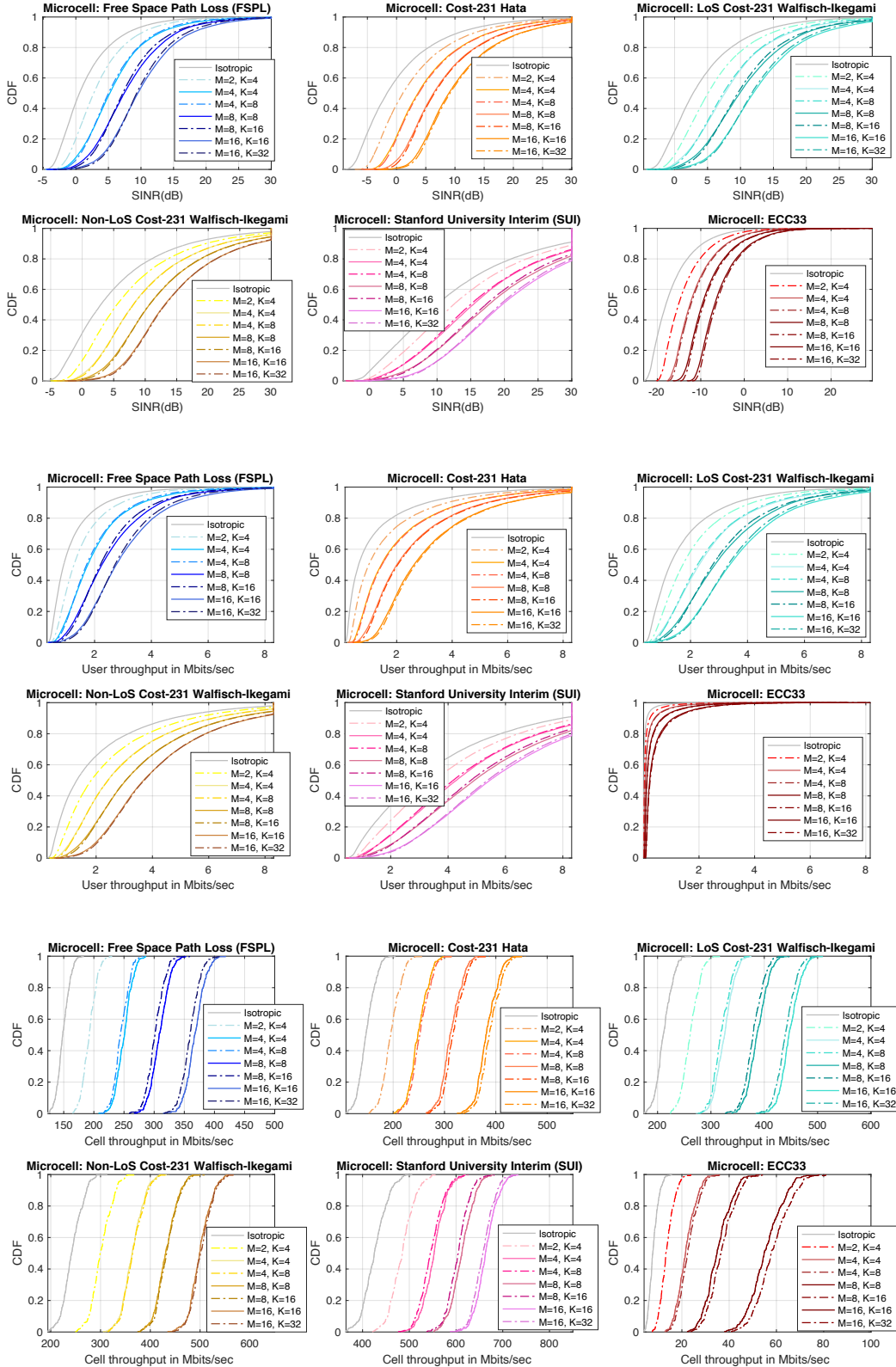




## Appendix B. Microcell simulation







## Appendix C. Array Factors polar plots

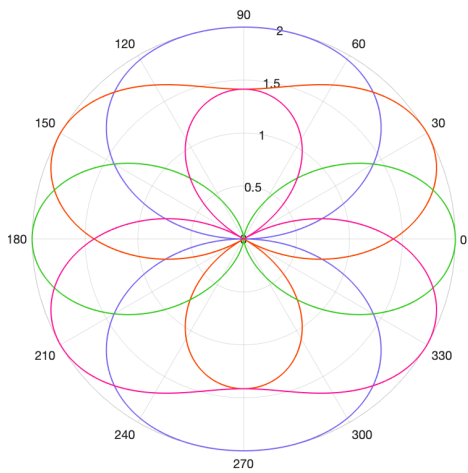


Figure 43 – 2 antenna elements, 4 beam patterns

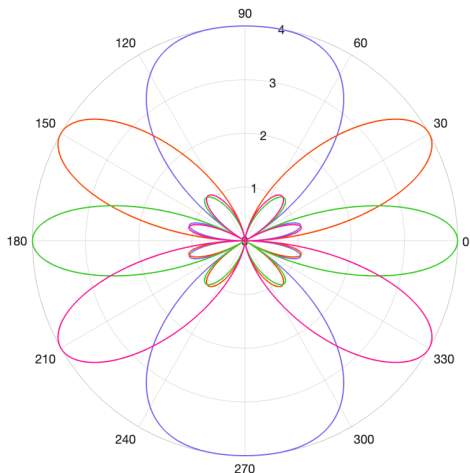


Figure 44 – 4 antenna elements, 4 beam patterns

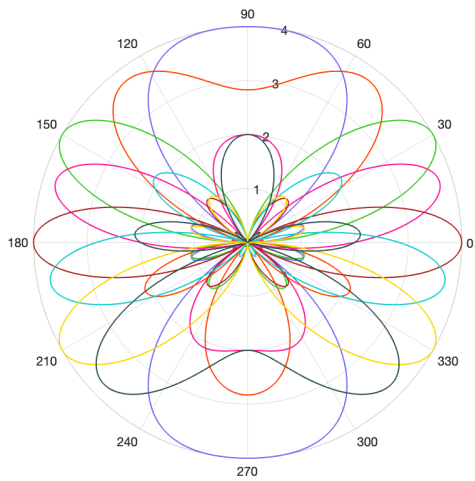


Figure 45 – 4 antenna elements, 8 beam patterns

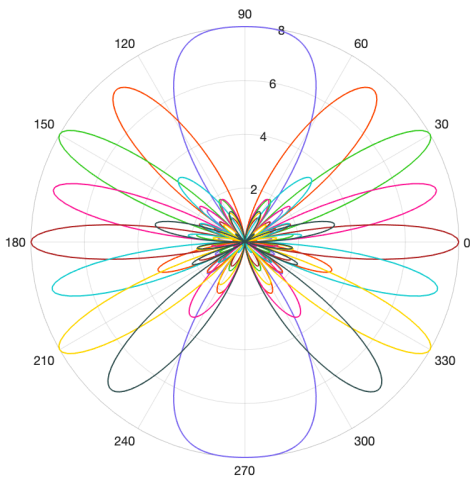


Figure 46 – 8 antenna elements, 8 beam patterns

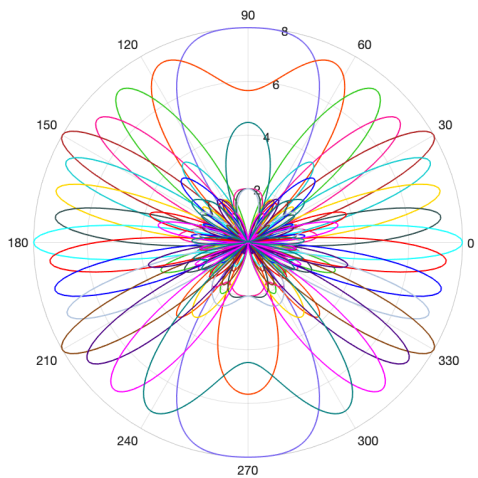


Figure 47 – 8 antenna elements, 16 beam patterns

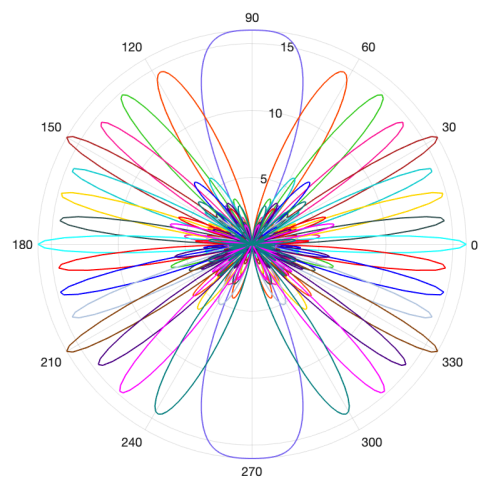


Figure 48 – 16 antenna elements, 16 beam patterns

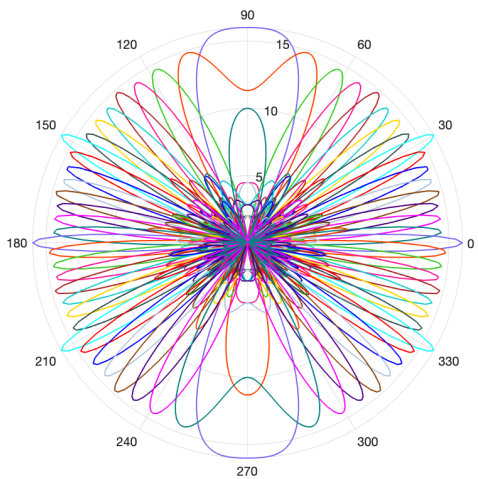


Figure 49 – 16 antenna elements, 32 beam patterns

## Appendix D.

### Software Traceability

The table below provides the list of all software used in this project, its authors and a brief description of its use. The code created by the student was developed using MATLAB 2019 and has not been tested on other versions of MATLAB – please use this version to ensure compatibility.

<b>Filename/Algorithm /Package</b>	<b>Author</b>	<b>Use</b>
<b>MATLAB R2019b</b>	Mathworks	Used for running the code and data analysis.
<b>rgb.m</b>	Kristján Jónasson Dept. of CS, University of Iceland (MATLAB)	Returns a Matlab RGB color specifier corresponding to a given color name. Obtained from: Mathworks file exchange <a href="https://www.mathworks.com/matlabcentral/fileexchange/1805-rgb-m">https://www.mathworks.com/matlabcentral/fileexchange/1805-rgb-m</a>
<b>main.m</b>	Student written (MATLAB)	Main function. Runs the simulation by calling all the other functions and plotting the data.
<b>randomColour.m</b>	Student written (MATLAB)	Returns a random colour (which is then used as the colour of the hexagonal layout).
<b>dbm2pow.m</b>	Student written (MATLAB)	Returns the corresponding linear value of power (Watts) for a given decibel-milliwatt (dBm) value. Inspired by the MATLAB db2pow function.
<b>pow2dbm.m</b>	Student written (MATLAB)	Returns the corresponding decibel-milliwatt (dBm) value for a given linear value of power (Watts). Inspired by the MATLAB pow2db function.
<b>patchplot.m</b>	Student written (MATLAB)	Patches (plots a filled polygonal region) and plots the centre of the polygon, denoted by a '+' sign. The colour used for patching is chosen by randomColour.m

<b>FreeSpace.m</b>	Student written (MATLAB)	Calculates the Free Space path loss as discussed in Section 2.8.1.
<b>OkumuraHata.m</b>	Student written (MATLAB)	Calculates the path loss according to the Okumura-Hata model as discussed in Section 2.8.2
<b>Cost231Hata.m</b>	Student written (MATLAB)	Calculates the path loss according to the Cost-231 Hata model as discussed in Section 2.8.3.
<b>Cost231WalfishIkegami.m</b>	Student written (MATLAB)	Calculates the path loss according to the Cost-231 Walfish-Ikegami model (LoS or non-LoS) as discussed in Section 2.8.4.
<b>SUI.m</b>	Student written (MATLAB)	Calculates the path loss according to the Stanford University Interim (SUI) model as discussed in Section 2.8.5.
<b>ECC33.m</b>	Student written (MATLAB)	Calculates the path loss according to the ECC-33 model as discussed in Section 2.8.6.
<b>PickCell.m</b>	Student written (MATLAB)	Gathers user input related to the cell by using a user-interface dialog box, allowing the reader to change the default settings. As seen in Figure 10.
<b>UserInput.m</b>	Student written (MATLAB)	Gathers user input of other parameters a user-interface dialog box, allowing the reader to change the default settings. As seen in Figure 11.
<b>checkboxPLmodels.m</b>	Student written (MATLAB)	Opens a user interface check box, allowing the reader to change the default settings of models ticked and their environment settings by pressing on the radio buttons. As seen in Figure 12.
<b>distanceangle.m</b>	Student written (MATLAB)	Calculates the Euclidean distance between the BS and the UE and the azimuth angle of departure and angle of arrival as discussed in Section 3.3.2 and 3.3.4.
<b>linkbudget.m</b>	Student written (MATLAB)	Calculates the received power as explained Sections 2.6.

<b>sumInter.m</b>	Student written (MATLAB)	Calculates the sum of interfering received power from other cells as mentioned in Section 3.3.6, using linkbudget.
<b>SNR_SINR.m</b>	Student written (MATLAB)	Calculates the SNR and SINR as explained in Sections 2.2-2.3, using linkbudget.
<b>Throughputs.m</b>	Student written (MATLAB)	Calculates the limited SINR (limited to 30dB), bandwidth efficiency, user and cell throughputs as explained in Sections 2.4-2.5, using linkbudget.
<b>calculateMK.m</b>	Student written (MATLAB)	Calculates all performance metrics for a given M and K to keep the main file size to a minimum – it calls sumInter, SNR_SINR, and Throughputs.
<b>beamforming3c720.m</b>	Student written (MATLAB)	Performs beamforming as described in Section 3.3.5. Plots the polar plot of the array factors versus angle for all beam patterns.
<b>ifplot.m</b>	Student written (MATLAB)	Plots the path losses of the models selected in checkboxPLmodels.m versus distance.
<b>ifeCDF.m</b>	Student written (MATLAB)	Plots the CDF of the metric determined. This metric is plotted for each of the models selected in checkboxPLmodels.m.
<b>isequal_legendfinal.m</b>	Student written (MATLAB)	Adds the legend of ifplot.m and ifecdf.m according to the models selected in checkboxPLmodels.m.
<b>plotecdf.m</b>	Student written (MATLAB)	Plots the CDF of the metric determined. Creates a subplot for each model selected in checkboxPLmodels.m.
<b>plotHEATMAPmodel.s.m</b>	Student written (MATLAB)	Plots the heatmap of the hexagonal cellular layout, using the specified performance metric. Creates a subplot for each model selected in checkboxPLmodels.m.
<b>pickModel.m</b>	Student written (MATLAB)	Opens a user interface window, allowing the reader to pick ONE propagation path loss models. by pressing on the radio buttons.

---

<b>plotBeamPatterns.m</b>	Student written (MATLAB)	Plots the polar plot of the array factors versus angle for each beam pattern as a subplot.
<b>FSPLpic.m</b>	Student written (MATLAB)	Plots Figure 4.
<b>barminmaxmeanCAS ES.m</b>	Student written (MATLAB)	Plots bar plots showing the minimum, maximum and mean values of the chosen metric for the Cases using the model selected in pickModel.
<b>barminmaxmeanMK. m</b>	Student written (MATLAB)	Plots bar plots showing the minimum, maximum and mean values of the chosen metric for the M and K values using the model selected in pickModel.
<b>barminmaxmeanRXT X.m</b>	Student written (MATLAB)	Plots bar plots showing the minimum, maximum and mean values of the chosen metric for the double-directional results using the model selected in pickModel.

---

